Single Event Microkinetic modelling for hydroisomerization and hydrocracking of n-Heptane

Nilaya Thote

https://commons.wikimedia.org/wiki/File:Oilrefinery-evansville,wy.jpg

TU Delft Delft University of Technology

Challenge the future

Single Event Microkinetic modelling for hydroisomerization and hydrocracking of n-Heptane

by

Nilaya Thote

in partial fulfillment of the requirements for the degree of

Master of Science
in Chemical Engineering

at the Delft University of Technology,
to be defended publicly on Friday July 7, 2017 at 10:30 AM.

Supervisor:	Prof. dr. ir. Thijs. Vlugt	TU Delft
Daily supervisor:	Ali. Poursaeidesfahani.	TU Delft
Thesis committee:	Dr. Freek. Kapteijn.,	TU Delft
	Dr. Johan. Grievink.,	TU Delft

TU Delft Delft University of Technology

”It matters not what someone is born, but what they grow to be.”

Albus Dumbledore

Abstract

With increasing environmental concerns, gasoline and lubricant oils with high octane number are being preferred as they result in reduced emissions from vehicles. Octane number of high molecular weight hydrocarbons can be increased by selectively isomerizing and cracking them into low molecular weight hydrocarbons. Catalytic hydroisomerization and hydrocracking is an important process to selectively branch and crack high molecular weight hydrocarbons in the petroleum industry. Research in modelling of these reactions is primarily based on characterizing and quantifying the vast network of reactions taking place in hydroisomerization and hydrocracking. This particular work focuses on reaction modelling of hydroisomerization and hydrocracking of n-Heptane in bifunctional catalysts based on Single Event Microkinetic (SEMK) approach. SEMK is a novel approach, which takes into account every fundamental step occurring in the vast reaction network and accounts for contribution of each of these steps to overall reaction rate. Results obtained via modelling by SEMK approach were fitted to experimental results in order to obtain estimates of rate constants of elementary steps.

An SEMK based model was created in three phases: reaction network generation, obtaining kinetic coefficients via SEMK model and development of rate equations and reactor model. The concentrations of individual species obtained from the model were fitted into experimental results to get estimations of kinetic rate coefficients of elementary steps. Estimations of these coefficients were obtained at three different temperatures (519K, 531K and 544K). A thorough analysis of results was performed in three parts. In the first part, the mass balance across the reactor is observed to ensure credibility of results obtained under steady state reactor conditions. In the second part, the product distribution of all components across the reactor was analyzed and compared with experimental results. It was observed that the product profiles fitted well with experimental observations for species formed in considerable amounts. In the third part, estimations of kinetic rate coefficents were obtained and compared with literature trends. It was observed that the parameters mostly followed literature trends. In the end recommendations are provided for overcoming the shortcomings of the present model for future study.

Acknowledgement

I would like to thank my supervisor **Prof.Dr.ir.Thijs Vlugt** for his support and for providing me with all the resources that were needed during this thesis work. His enthusiasm while discussing a problem statement motivated me to take up this project and successfully carry it to the end.

My sincere gratitude to my daily supervisor, MSc. **Ali Poursaeidesfahani** for helping me during each stage of this thesis project. I am thankful to him for providing me with his valuable suggestions and comments, without which completion of this work would not have been possible.

Moreover, I would like to thank my friend **Rahul Dhopeshwar** for helping me in almost anything and everything during my entire Master's education. He encouraged me during down time of this project. I am also grateful to my friends **Sameer, Prajakta, Rucha, Sakshi, Arjun and Kshiteej** for always supporting me and providing valuable inputs.

Moreover, I would like to thank **my family (Niranjan Thote, Neha Thote and Sakshi Thote)** for supporting me in all the situations. Their trust has always motivated me to give my best performance.

List of Figures

List of Tables

List of Symbols

Symbol	Description
k	Kinetic coefficient of rate of reaction of any elementary step
k_{b}	Boltzmann constant
T	Temperature
h	Planck's constant
ΔS^{o}	Change in entropy of a reaction
R	Gas constant
ΔH^{o}	Change in enthalpy of a reaction
$S^{\mathrm{o}}_{\mathrm{ExtRot}}$	Contribution of external rotation to entropy
$\hat{S}^{\mathrm{o}}_{\mathrm{ExtRot}}$	Intrinisic contribution of external rotation to entropy
σ_{Ext}	External symmetry number
$S^{\mathrm{o}}_{\mathrm{IntRot}}$	Contribution of internal rotation to entropy
$\hat{S}^{\mathrm{o}}_{\mathrm{IntRot}}$	Intrinisic contribution of internal rotation to entropy
σ_{Int}	Internal symmetry number
$S^{\mathrm{o}}_{\mathrm{Rot}}$	Rotational contribution to entropy
$\hat{S}^{\mathrm{o}}_{\mathrm{Rot}}$	Intrinsic rotational contribution to entropy
α	alpha position of atom
β	beta position of atom
$n_{\alpha\mathrm{H}}$	Number of Hydrogen atoms in α position with respect to positively charged carbon atom
$n_{\alpha\mathrm{Me}}$	Number of Methyl groups in α position with respect to positively charged carbon atom
$n_{\beta\mathrm{H}}$	Number of Hydrogen atoms in β position with respect to positively charged carbon atom
$\sigma^{\mathrm{R}}_{\mathrm{gl}}$	Global symmetry number of reactant
$\sigma^{\neq}_{\mathrm{gl}}$	Global symmetry number of activated complex
$\Delta\hat{S}^{\mathrm{o}}$	Change in intrinsic activation energy
n_{e}	Number of single events of reaction
z, z_1, z_2	Represents secondary (s) or tertiary (t) carbenium ion
$k_{\mathrm{pr}}(\mathrm{z})$	Kinetic coefficient for protonation into carbenium ion of character z (in $\frac{\mathrm{kg_{cat}}}{\mathrm{kmol.s}}$)
$k_{\mathrm{hs}}(\mathrm{z}_1;\mathrm{z}_2)$	Kinetic coefficient for hydride shift of ion of character z_1 into ion of character z_2 (in s^{-1})
$k_{\mathrm{ms}}(\mathrm{z}_1;\mathrm{z}_2)$	Kinetic coefficient for methyl shift of ion of character z_1 into ion of character z_2 (in s^{-1})
$k_{\mathrm{pcp}}(\mathrm{z}_1;\mathrm{z}_2)$	Kinetic coefficient for PCP decomposition of ion of character z_1 into ion of character z_2 (in s^{-1})
$\mathrm{O}_{\mathrm{ref7}}$, $\mathrm{O}_{\mathrm{ref4}}$, $\mathrm{O}_{\mathrm{ref3}}$	Reference olefin for hydrocarbon with carbon number 7, 4 and 3 respectively
$k_{\mathrm{de}}(\mathrm{z};\mathrm{O}_{\mathrm{ref}})$	Kinetic coefficient for deprotonation of ion of character z into reference olefin (in s^{-1})
$k_{\mathrm{cr}}(\mathrm{R}_1;\mathrm{R}_{\mathrm{cr1}},\mathrm{O}_{\mathrm{cr1}})$	Kinetic coefficient for cracking of ion R_1 into ion $\mathrm{R}_{\mathrm{cr1}}$ and olefin $\mathrm{O}_{\mathrm{cr1}}$ (in s^{-1})
$k_{\mathrm{iso}}(\mathrm{z}_1;\mathrm{z}_2)$	Kinetic coefficient for isomerization of ion of character z_1 into ion of character z_2 (in s^{-1})

Symbol	Description
$k_{\mathrm{h}}(\mathrm{o};\mathrm{p})$	Kinetic coefficient for hydrogenation of olefin o into paraffin p
$k_{\mathrm{dh}}(\mathrm{p};\mathrm{o})$	Kinetic coefficient for dehydrogenation of paraffin p into olefin o
R_{k}^{+}, $R_{\mathrm{m}}^{+}, R_{\mathrm{p}}^{+}$, $R_{\mathrm{l}}^{+}, R_{\mathrm{o}}^{+}$, R_{n}^{+}	Carbenium ions of type k, m, p, l, o and n
$K_{\mathrm{iso}}(O_{\mathrm{ref}} \leftrightharpoons O_1)$	Equilibrium constant for isomerization of reference olefin to olefin O_1
$\Delta G_{\mathrm{iso}}^{\mathrm{o}}$	Change in Gibbs free energy during isomerization reaction
$\Delta H_{\mathrm{iso}}^{\mathrm{o}}$	Change in enthalpy during isomerization reaction
$\Delta S_{\mathrm{iso}}^{\mathrm{o}}$	Change in entropy during isomerization reaction
P_{gas}	Any paraffin P in gas phase
Eq	Equilibriated reaction
P_{adsorbed}	Any paraffin P in adsorbed phase
$P_{\mathrm{i,adsorbed}}$	Paraffin of species i in adsorbed phase
$q_{\mathrm{s,i}}$	Concentration of paraffin of species i in adsorbed state
$q_{\mathrm{sat,i}}$	Saturated concentration of paraffin of species i in adsorbed state
b_{i}	Langmuir isotherm parameter for paraffin i
p_{i}	Partial pressure of paraffin i
O_{ij}	Olefin of type j derived from paraffin of species i
K_{eq}	Equilibrium constant
$C_{O_{\mathrm{ij}}}$	Concentration of Olefin O_{ij} (in $\frac{\mathrm{kmol}}{\mathrm{kg_{cat}}}$)
C_{R^+}	Concentration of carbenium ion R^+ (in $\frac{\mathrm{kmol}}{\mathrm{kg_{cat}}}$)
C_{H^+}	Concentration of free acid sites in catalyst (in $\frac{\mathrm{kmol}}{\mathrm{kg_{cat}}}$)
C_{t}	Concentration of total acid sites (in $\frac{\mathrm{kmol}}{\mathrm{kg_{cat}}}$)
$C_{P_{\mathrm{i,adsorbed}}}$	Concentration of Paraffin P_{i} in adsorbed phase (in $\frac{\mathrm{kmol}}{\mathrm{kg_{cat}}}$)
$R_{P_{\mathrm{i}}}$	Net rate of formation of Paraffin P_{i} (in $\frac{\mathrm{kmol}}{\mathrm{kg_{cat}}.s}$)
$R_{O_{\mathrm{ij}}}$	Net rate of formation of Olefin O_{ij} (in $\frac{\mathrm{kmol}}{\mathrm{kg_{cat}}.s}$)
ρ_{cat}	Density of catalyst ($\frac{\mathrm{kg_{cat}}}{\mathrm{m^3}}$)
ϵ	Porosity of catalyst
$p_{\mathrm{i}}^{\mathrm{n+1}}$	Partial pressure of paraffin species at node n+1
$p_{\mathrm{i}}^{\mathrm{n}}$	Partial pressure of paraffin species at node n
L	Total length of reactor
n_{t}	Total number of nodes in reactor

Contents

1

Introduction

In the petroleum industry, there is an excessive demand for cleaner fuels with high energy efficiency. It has been observed that diesel fuels produced by Fischer-Tropsch (FT) process exhibit excellent properties like high cetane number (typically above 70), diminished amounts of sulfur, nitrogen and aromatics. Hence, these fuels result in reduced emissions of pollutants from the engine [1]. FT processes produce a wide span of carbon numbers ranging from C_1 to $C_{21}+$. The heavier products of FT processes form major source of feedstocks for petrochemical products like lubricating oils and kerosene [1]. These heavy product components from FT processes usually contain long chain waxes and paraffins. Also, petroleum feedstocks contain long and linear alkanes of varying carbon numbers. All these long chain alkanes need to be selectively branched and converted to smaller chain alkanes in order to increase the octane number of gasoline and low temperature properties of diesel and lubricating oils [2–5]. The chemical treatment for achieving this is called catalytic hydroisomerization and hydrocracking. Hydroisomerization is selective branching of linear alkanes into branched isomers. Whereas, hydrocracking is breaking of linear alkanes into lower molecular weight alkanes. Bifunctional catalysts are used for these chemical treatments [1]. Bifunctional catalysts are a particular set of hydrogenation catalysts which contain both, Lewis metal base sites and Brønsted acid sites [6].

Since past few decades, owing to the rising environamental concenrs a lot of research is being carried on hydrocracking and hydrotreating processes [7–11]. Research has mainly been focused on two aspects: higher catalytic efficiency and better quantification of reaction kinetics. The studies strive for superior comprehension of isomerized and cracked product distribution so as to achieve desired product properties. Various approaches have been developed so far to improve understanding of reaction kinetics of hydroisomerization and hydrocracking [12–15]. This process usually contains an input feed of long chain alkanes and output of products comprising a distribution of multiple isomers and low molecular weight cracked products. To produce fuel of higher grade, selective isomerization with a particular product distribution is required [16]. Hence reaction models are needed which can help in designing reactors with desired product distributions. Due to multiplicity of reactions and components involved, efforts are put to simplify the model to a maximum extent while maintaining the accuracy of the model. Major types of reaction models developed so far are based on Lumping, Continuous Lumping and Mehchanistic approaches [6, 17, 18].

In literature, early studies of catalytic hydrocracking of complex feedstocks were mostly focused on development of lumped kinetic models. In these models, feedstock is divided into psuedocomponents known as 'lumps'. These lumps are formed of components on the basis of their boiling point range, degree of branching in components, carbon number, molecular weight etc [19–21]. For example, Steijns and Froment have considered reversible hydroisomerization reaction network as in Scheme 1.1 for their work on kinetic analysis of hydrocracking of n-Decane and n-Dodecane [22]. For the simplified reaction network in Scheme 1.1, rate constants for global conversion of lumps are considered for rate expressions of lumped species.

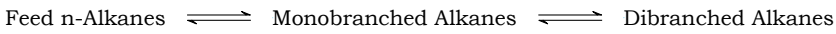

Scheme 1.1: Reaction Scheme for lumped kinetic approach to hydroisomerization of n-Alkane by Steijns and Froment [22]

On the basis of boiling point ranges, Weekman and Nace gave reaction scheme as in Scheme 1.2 for fluidized catalytic cracking of charged gas oil (C_1) into gasoline boiling fraction at 410°F (C_2) and remaining fraction of butanes, dry gas and coke (C_3) [23].

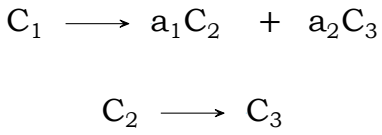

Scheme 1.2: Reaction Scheme for lumped kinetic approach to catalytic cracking of charged gas oil by Weekman and Nace [23]

A more detailed lumped model of 10 lumps is considered by Jacob et al. for fluidized catalytic cracking of feedstock charge into gasoline, light products, heavy fuel oil and light fuel oil [17]. Stangeland considered a model comprising of feedstock lumps in a series of 50°F range of cuts in boiling points. Herein, it is assumed that every heavier cut cracks into a lighter cut of lumps [24]. In order to achieve more accuracy in models, greater number of lumps were considered by researchers. As the number of lumps increases in model, the number of parameters to be estimated also increase and this increases the computational complexity. Another major shortcoming of lumped model is the dependence of kinetic parameters on composition of feedstock. Hence for each different input feedstock, new set of parameters have to be estimated [11].

All of the above mentioned works have been based on discrete lumping approach. Laxminarasimhan et al. developed a model for hydrocracking of vaccum gas oil based on continuous lumping approach [18]. In this model, the rate constant for hydrocracking is formulated as a continous monotonic function of true boiling points of components in the mixture at a particular time. Along the length of reactor, more heavy components are cracked into lighter components and the true boiling point of mixture changes. Hence the rate constant in this model is a monotonic function of residence time. Both dicrete and continuous lumping approach, however, do not take into account the fundamental chemistry of reactions taking place in hydroisomerization and hydrocracking. In these models, rate constants are estimated solely on the basis of observed conversions between lumps. This drawback of lumping models highlights the need for development of mechanistic models.

Mechanistic models take into account the chemistry of individual components and reactions in a network. Liguras et al. tried to overcome the shortcomings of lumping models by considering mechanistic aspects of reaction chemistry. They further divided lumps of normal, branched and cyclic paraffins into carbon centers [25]. Rates of reactions involving these carbon centers were modelled as functions of carbon number and position. Quann et al. developed a new model known as 'Structural-Oriented Lumping' to describe composition and reactions in complex hydrocarbon mixtures. In this model, a hydrocarbon molecule is represented as a vector of structural features in increasing order. To represent a mixture of hydrocarbons, a set of these vectors is considered with associated weight percentage of each vector [26].

For all the models described till now, the major hindrance to their application for industry scale is their specificity to simple feedstocks and non-accountibility of elementary carbon chemistry taking place during the process [27]. To tackle the former problem in case of lumped models, more lumps can be introduced into the model. However complex mixtures in industrial processes involve large number of lumps. Taking into account all the different lumps adversely affects the simplicity of model. Also for lumped models, the existence of multiple routes for conversion between two lumps limits the model to represent complicated reaction network. In case of structural mechanistic modelling, these models are less capable of adapting to complex feed mixtures of arbitrary compositions and are hence plagued by specificity.

In the vast network of reactions taking place inside the bifunctional catalyst, every step has a finite contribution towards reaction rate. In order to account for every step, Froment et al., developed a kinetic modelling approach comprising of all elementary steps using chemistry of carbenium ions [6, 27]. This approach is called as 'Single Event Microkinetic' (SEMK) model. As this model accounts for all individual steps, the number of unknown parameters for a SEMK model in case of hydroisomerization and hydrocracking of single n-Alkane feed will be much greater than those in case of lumped model for the same. However in case of complex feeds, as the number of elementary steps is limited in number, the same elemnetary steps will be encountered repeatedly and hence the number of unknown parameters will not increase much. Therefore in case of complex feeds the number of unknown parameters in SEMK model will be almost same or less than those in lumped models. Based on boolean matrices approach developed by Clymans et al.[28] and Hillewaert et al. [29], Baltanas et al. devised a method to generate reaction network in hydroisomerization and hydrocracking via a computer algorithm [30]. Vynckier et al. extended the SEMK model for single feed alkanes to complex feedstocks by introducing lumping in elementary kinetics [6]. Svoboda et al. determined rate parameters for hydroisomerization and hydrocracking of n-Octane using SEMK model [31]. Martens et al. used SEMK to model hydrocracking of C_8-C_{12} paraffins of Pt/USY zeolites [15]. Park et al. incorporated Evans-Polanyi relationship with SEMK model to reduce parameters using thermodynamic contraints for conversion of methanol to olefins [32]. Martinis et al. used the same approach for alkylation of isobutane with butenes [33].

In this work, SEMK approach is used to investigate the reaction mechanism and product distributions of hydroisomerization and hydrocracking of n-Heptane. The reactions are carried out on bifunctional catalyst of zeolite framework type BEA. This particular catalyst has been chosen due to its large pore size and hence minimum diffusive effects and shape selectivity on products. In this work, firstly a reaction network and kinetic model is developed based on the SEMK approach to quantify net rates of formation of different isomers and cracked products. Next, the model is fitted to experimental results provided by our industrial partner and estimation of rate constants for reactions is obtained. Furthermore, the product distributions are studied and compared with experimental results and trends in literature.

2

Model

In case of Single Event Microkinetic Model (SEMK) for hydroisomerization and hydrocracking of n-alkane in a bifunctional catalyst, rate equation pertaining to every elementary step in the reaction network is taken into account. Every elementary step has a finite contribution towards the overall reaction. As the overall reaction consists of multiple elementary steps, modelling of rate constants of these steps will demand large amount of computations. The SEMK model hepls to mitigate this problem to a large extent. In this chapter, a model is developed using the SEMK approach in which all elementary steps in hydroisomerization and hydrocracking of n-heptane are taken into account. In first section of this chapter, an algorithm is developed to store and account for every elementary step in the reaction network. Next, rate constant governing rate equation of each step is identified. Thermodynamic constraints are used to then reduce the number of independent rate constants for all steps. As mentioned earlier, the last section develops an overall rate equation by obtaining net rate of formation of each species in the network using independent rate constants derived in previous section.

The development of model is divided into following stages:

1. Reaction network generation
2. Kinetic coefficient via Single Event Micro-Kinetic (SEMK) model
3. Development of rate equations and reactor model

2.1. Reaction Network Generation

In this section, a reaction network is generated on computer by using the approach first developed by Baltanas and Froment [30]. First, a method is deviced to store species molecules in the network. Then, algorithms are developed for carrying out elementary steps on each molecule via suitable operation method. Lastly, all the individual elementary steps are compiled together in a bigger network algorithm to generate an interconnected web of hydroisomerization and hydrocracking reactions.

2.1.1. Species Storage

To account for every elementary step taking place in the reaction network, it is necessary to have a database of all reactions taking place in the catlalyst and respective species involved in these reactions in a relevant form. This is achieved by storing every molecule species in either of the two forms: Boolean Matrix (BM) form and Standardized Vector (SV) form [30]. In the case of BM, all elementary reactions can be easily performed on molecules via boolean matrix operations. As a large amount of memory space is required to store BM's, storage of species is preferred in the form of SV [30]. In this form, a molecule is tored in the form of a vector consisting two arrays. The first array stores character of each carbon atom (1=primary,

2=secondary, 3=tertiary, 4=quarternary) and second array stores nature of carbon atoms as given by conventions in Table 2.1 [6]. The SV form especially helps when dealing with more complex aromatic and naphthenic spcies or longer chain hydrocarbons [6].

Table 2.1: Conventions to denote nature of carbon atoms in Standardized Vector (SV) form for storage of molecules. The SV representation of hydrcarbon molecules is suitable for high molecular weight hydrocarbons as compared to the Boolean Matrix (BM) representation (described in Figure 2.1) due to its requirement of low storage space as compared to BM form.

Index	Nature of atom
1	aromatic carbon atom
2	naphthenic carbon atom part of double bond
3	other naphthenic carbon atom
4	acyclic carbon atom part of double bond
5	other acyclic carbon atom

For an efficient execution of reaction network, all hydrocarbons should be stored in SV form and while performing elementary reactions, the SV should be converted into BM. Matrix operations should then be carried out on BM to obtain the product. The formed product should be stored again in SV form. The focus of present work is on hydroisomerization and hydrocracking of n-heptane, which involves not more than 12 paraffin species. Furthermore, the entire network algorithm requires a run time of few minutes. Therefore, due to the low memory requirement and limited run time, all the storage and matrix operations are performed on BMs' in this work. However, for hydrocracking and hydroisomerization of an input of complex range of species, species should be stored in SV form and elementary steps should be performed in BM form [6].

Boolean Matrix (BM)

A Boolean Matrix (BM) or Binary Matrix contains all its elements in the boolean domain i.e. in domain $\{0, 1\}$. In the BM form, an n-Heptane molecule is represented as given in Figure 2.1. In this figure, n-Heptane molecule is represented in the form of Matrix A. The presence or absence of bond between atom i and j is given by the value of element A_{ij} in the matrix as 1 or 0. For example, in BM representation of n-Heptane molecule in Figure 2.1, atom 2 is bonded to atoms 1 and 3. Hence elements $A_{12} = A_{21} = A_{23} = A_{32} = 1$. Similarly, atom 2 is not bonded to any atom other than 1 and 3. Hence in second row of matrix A, all the elements other than A_{21} and A_{23} are zero. The primary, secondary, tertiary or quarternary nature of an atom i is given by the number of non-zero elements in row i of BM. Hence the BM for a general molecule is defined as in Equation 2.1.

=

	1	2	3	4	5	6	7
1	0	1	0	0	0	0	0
2	1	0	1	0	0	0	0
3	0	1	0	1	0	0	0
4	0	0	1	0	1	0	0
5	0	0	0	1	0	1	0
6	0	0	0	0	1	0	1
7	0	0	0	0	0	1	0

Figure 2.1: Boolean Matrix (BM) representation of n-heptane molecule in the form of Matrix A in right hand side. The presence or absence of bond between atom i and j is given by the value of element A_{ij} in the matrix as 1 or 0. The BM form is used for carrying out computer generation of reaction network in this work. All the reactions are carried out as matrix operations on individual BM representations of carbenium ions, olefins and paraffins.

$$A_{ij} = A_{ji} = \begin{cases} 0 & if\ bond\ does\ not\ exist\ between\ atoms\ i\ and\ j \\ 1 & if\ bond\ exists\ between\ atoms\ i\ and\ j \end{cases} \tag{2.1}$$

Every BM is accompanied by an associated 2 element array [30]. This array consists of information about the presence of charge or double bond in the molecule. The associated array is defined as in Table 2.2.

Table 2.2: Description of Associated Array in BM representation of molecule. It consists of information about the presence of charge or double bond in the molecule. This array is essential to differentiate between carbenium ion, olefin and paraffin species.

Associated Array	Description
[0, r]	Carbenium ion where positive charge is on atom r
[s, t]	Olefin where the double bond is between atoms s and t

2.1.2. Matrix Operations for Elementary Reactions

Before devicing methods to perform matrix operations for elementary reactions on each stored species, it is important to identify the quasi-equilibriated and non-equilibriated elementary steps taking place inside catalyst. For an incoming stream of n-Heptane into catalyst bed inside reactor, n-Heptane, and other paraffins generated in later sections of the reactor, is first physisorbed into the pores of catalyst. This physisorbtion is modelled by means of Langmuir Isotherms. The physisorbed paraffins are dehydrogenated into olefins on metal sites of bifunctional catalyst. These olefins undergo protonation, isomerization, cracking and deprotonation in acid sites of bifunctional catalyst. Newly formed olefins as a result of all the reactions on acid sites, are hydrogenated to paraffins on metal sites and transported out of catalyst via desorption. It is assumed that catalyst has sufficient activity to quasi-equilibriate hydrogenation and dehydrogenation. The reactions taking place on acid sites are the elementary steps to be modelled as rates for these reactions depend on species involved as well as the type of reaction [6, 27]. Hence matrix operations are deviced for protonation, isomerization, cracking and deprotonation reactions to generate the network. These elementary reactions are presented in Schemes 2.1, 2.2, 2.3, 2.4, 2.6-2.10 and 2.11.

Protonation: Olefins, which are formed on metal sites as a result of dehydrogenation of paraffins, get protonated into carbenium ions on acid sites. Since primary carbenium ions are much less stable as compared to secondary and tertiary carbenium ions, formation of primary carbenium ions is not considered in any part of reaction network generation [27]. Protonation of every olefin will give two carbenium ions unless one of the cations formed is a primary carbenium ion. The protonation operation on stored species in BM form involves changing the first element of associated array to zero and changing the second element to appropriate ID of charged carbon. The code also takes care of prohibiting formation of primary carbon atoms.

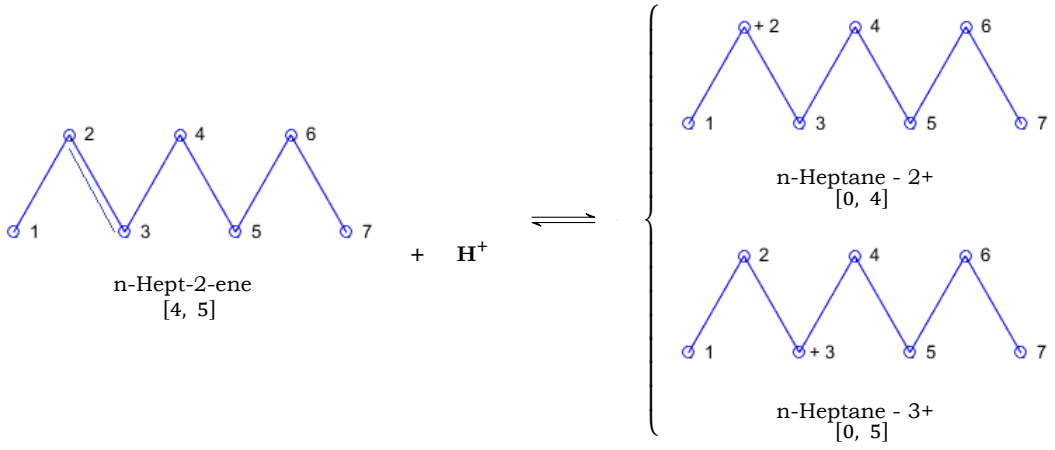

Scheme 2.1: Protonation reaction of n-Hept-2-ene

Hydride Shift: Hydride shifts are carbocation rearrangement reactions in which hydrogen atom attached to carbon in α position of positive charge migrates to the positively charged atom and hence charge is shifted to the perviously uncharged carbon atom in α position. Only hydride shifts in adjacent carbon atoms are considered in the network. Hydride shift is performed on BM by simply changing the ID of charged atom (element 'r' in Table 2.2) in the associated array.

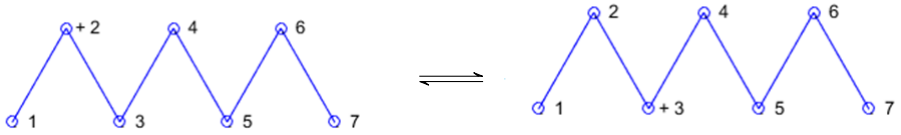

n-Heptane - 2+ n-Heptane - 3+

Scheme 2.2: Hydride shift reaction of n-Heptane - 2+

Methyl Shift: Methyl shift is carried out by type A isomerization in the present model. In this type of isomerization, the number of methyl branches in the molecule remain same [34]. Type A isomerization in computer algorithm is performed by checking the character of carbon in α position with respect to positive charge, whose position is stored in the associated array ([0, i] if charge is on atom i) of BM. Index of α carbon is obtained by checking non-zero elements of i^{th} row of BM. Primary, secondary, tertiary or quarternary character of α carbon is in turn obtained by checking for number of non-zero elements in the respective rows. Methyl shift is feasible if the nature of α carbon is either tertiary or quarternary. After checking nature of α carbon, if methyl shift is possible, the relevant rows and columns in the BM are changed along with the index of charged carbon in the associated array.

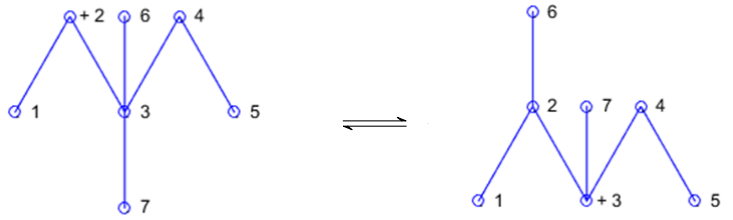

3,3-Dimethylpentane - 2+ 2,3-Dimethylpentane - 3+

Scheme 2.3: Methyl shift reaction of 3,3-Dimethylpentane - 2+

PCP Branching: Type B isomerization takes place via decomposition of Protonated Cyclopropane (PCP) ring. In this type of isomerization, the degree of branching changes in the molecule [34]. Index of β carbons with respect to positively charged carbon atom is required for PCP ring formation and decomposition. Positions of β carbons are obtained using the square normalized matrix of BM i.e $S = BM^2 - I$ [30]. The identity of β carbon with respect to any atom i is obtained by checking for non-zero elements in the i^{th} row of S. Only β carbon atoms which are not quarternary in nature are eligible for formation of PCP ring. If an eligible β carbon is detected, an activated complex of PCP ring is formed between charged atom, α carbon and β carbon. A range of products is formed as each bond in PCP ring is cleaved one at a time. The positive charge after bond cleavage is alotted to the carbon atom with higher degree of branching. In case both the atoms are of same nature, the charge is allocated to both the atoms with equal probability and as a result two products are formed. Provisions for appropriate PCP ring formation, bond scission and charge allocation can be made in the code and a range of product BMs' is obtained as given in example PCP decomposition of n-Heptane - 3+ in Figure 2.5. The code also makes provision to avoid formation of primary ions.

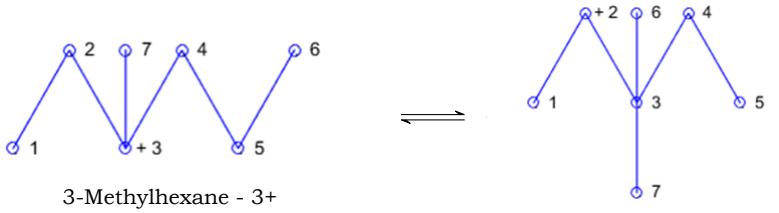

Scheme 2.4: PCP branching reaction of 3-Methylhexane - 3+

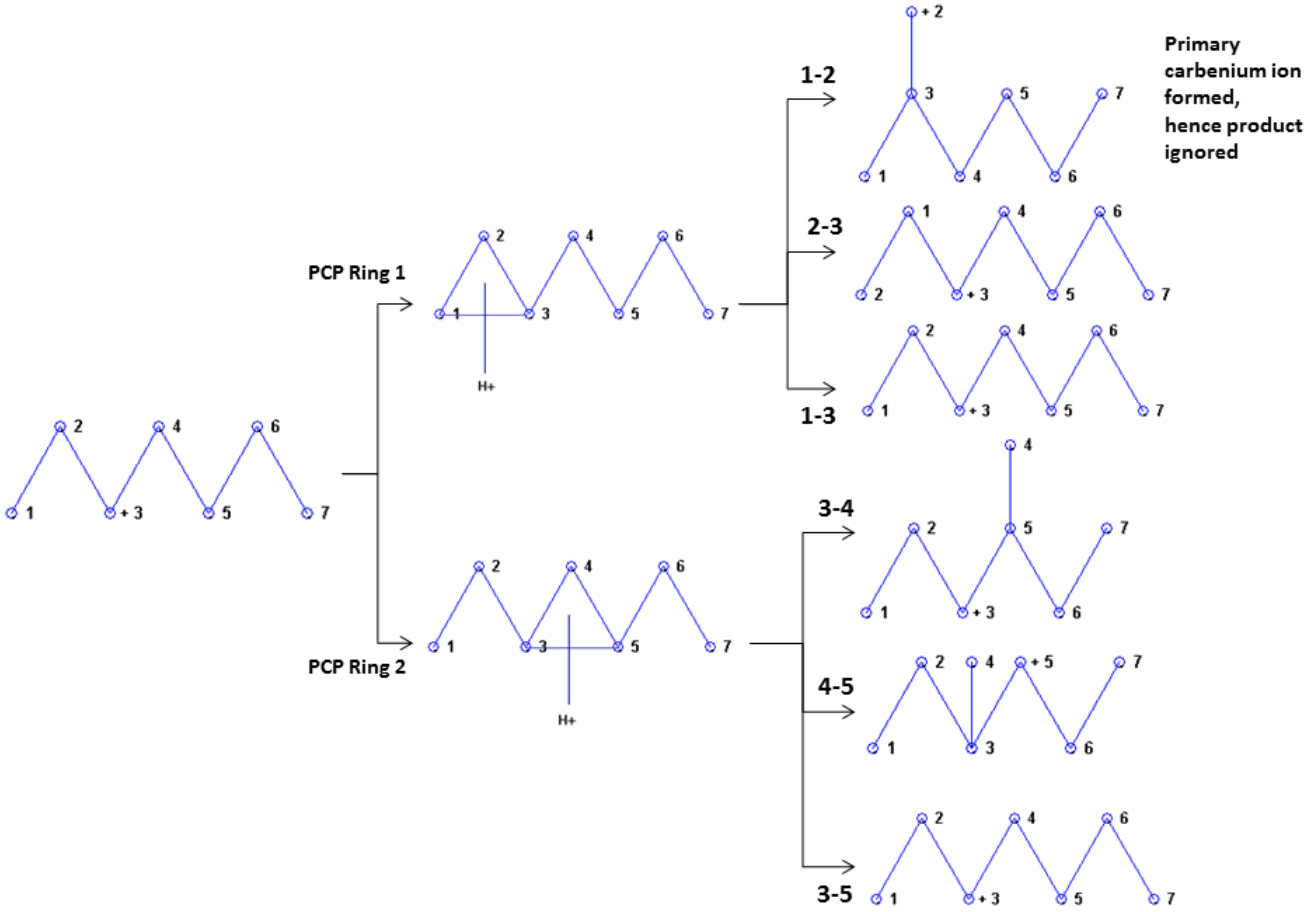

Scheme 2.5: Mechanism for PCP ring formation and decomposition of n-Heptane - 3+. In this reaction, PCP rings are first formed with eligible β carbon atoms with respect to charged carbon in carbenium ion. Each bond in the PCP ring is then selectively cleaved to form a range of products with less, same or more degree of branching with respect to the reactant molecule.

Cracking: In cracking, long-chain hydrocarbon molecules break into smaller fragments. Cracking takes place via β scission, wherein, the two electrons in the β C-C bond with respect to positive charge migrate towards the α C-C bond of positive charge. Thus this α C-C bond becomes unsaturated and the carbon in β position becomes electron deficient and attains positive charge [34]. The above mechanism is implemented in a computer code to facilitate output of two matrices of cracked molecules. β scission is classified into four types as : A, B_1, B_2, C and D. Type A mechanism involves three side chains on β carbon with respect to positive charge. This type of cracking results in formation of tertiary carbenium ion and alkene with one of the bonded atoms as tertiary carbon. Type B_1 and B_2 mechanisms result in formation of tertiary and secondary carbenium ions respectively. In type C mechanism, both of the cracked products have secondary carbon atoms. Type D mechanism leads to

formation of primary carbenium ions which is very unlikely and hence is not considered in cracking on $C_7H_{15}^+$. Only types B_1, B_2 and C are observed in cracking of $C_7H_{15}^+$ [34] and are implemented as matrix operations on $C_7H_{15}^+$ in the code. All the cracking reactions involved in present work are illustrated in Schemes 2.6, 2.7, 2.8, 2.9 and 2.10.

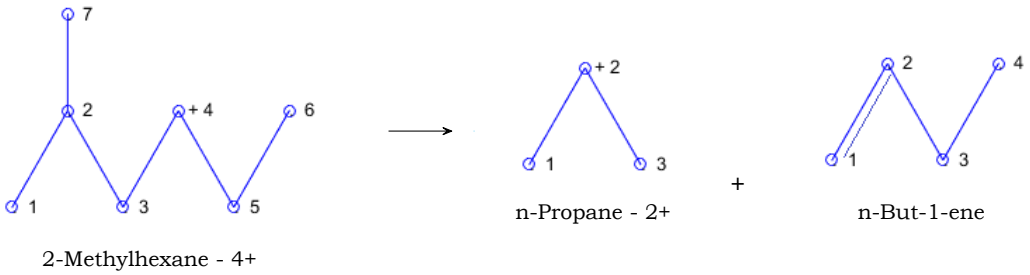

Scheme 2.6: Type C cracking of 2-Methylhexane - 4+

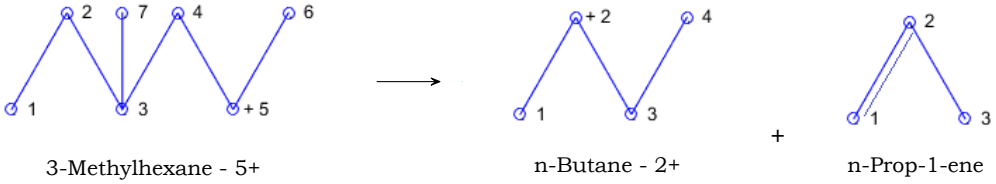

Scheme 2.7: Type C cracking of 3-Methylhexane - 5+

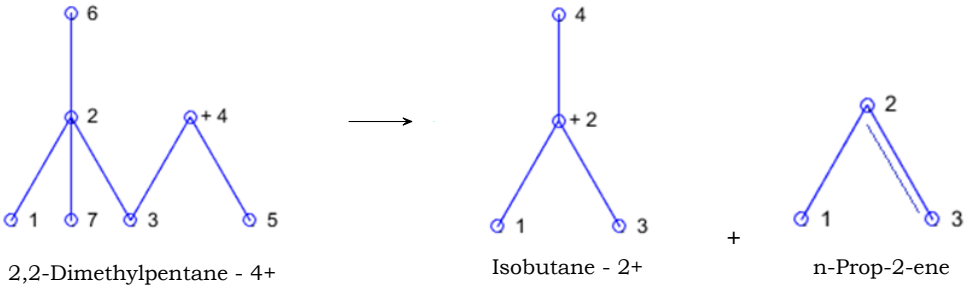

Scheme 2.8: Type B_1 cracking of 2,2-Dimethylpentane - 4+

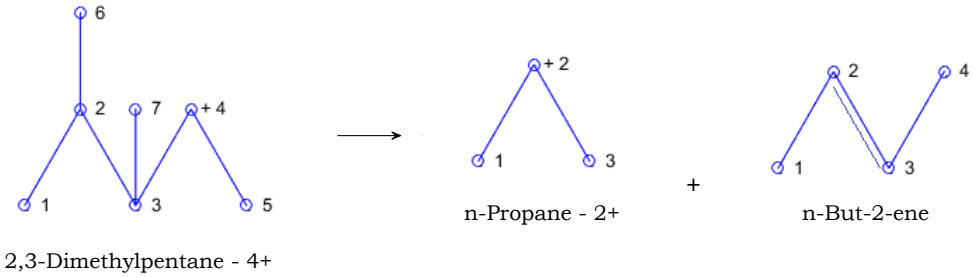

Scheme 2.9: Type C cracking of 2,3-Dimethylpentane - 4+

Deprotonation: Carbenium ions undergo deprotonation to form olefins. Like protonation, every deprotonation reaction can result in formation of two types of olefins. Similar to protonation, implementation of deprotonation in code also involves making required changes in associated matrix.

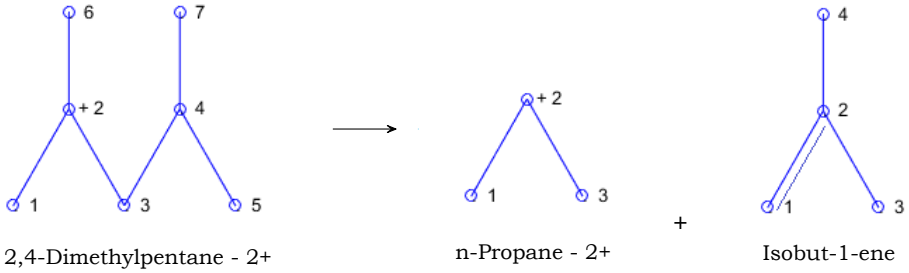

Scheme 2.10: Type B_2 cracking of 2,4-Dimethylpentane - 2+

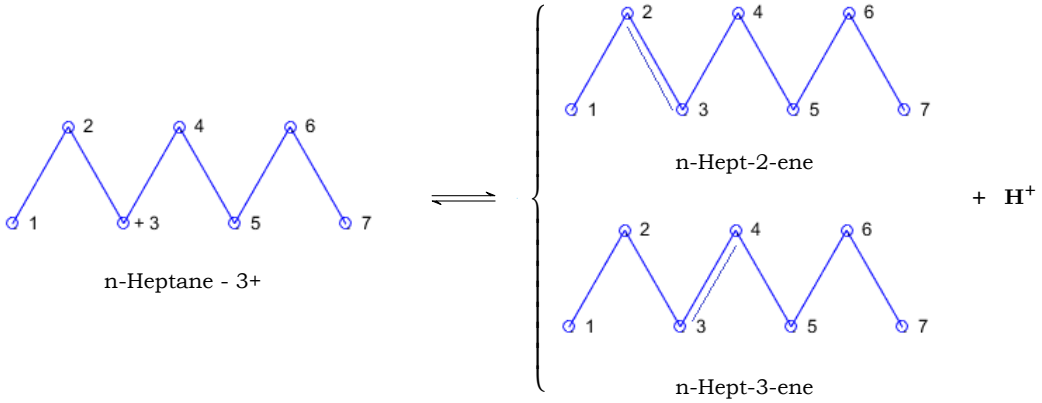

Scheme 2.11: Deprotonation reaction of n-Heptane - 3+

Standardized Matrices

During the execution of above elementary steps on matrices, the numbering order of atoms in molecule might get random, as seen in products of Figure 2.5, and different matrices may represent the same molecule. To solve this problem, a code was developed to convert every randomly numbered matrix into a standardized matrix in which atoms are numbered in a prioritized manner. While numbering, first priority is given to primary chain while the side chains are numbered according to their order of occurance on primary chain. An example of this is illustrated in Figure 2.2. After execution of every elementary step, the products are standardized and then stored in the database.

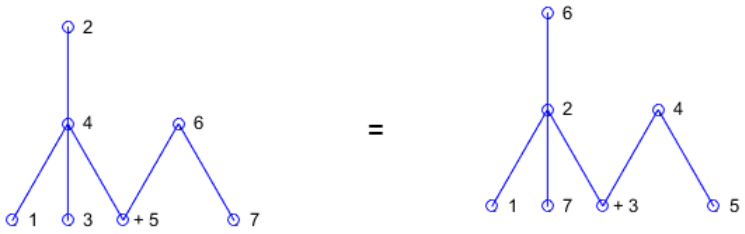

Figure 2.2: Standardized numbering of 2,2-Dimethylpentane for a standard Boolean Matrix representation. This standardized form of numbering was implemented into the algorithm to avoid different representation of same molecule.

2.1.3. Reaction Network Algorithm

All the elementary steps described in Section 2.1.2 are carried out sequentially on each of the involved species according to a Network Algorithm described in Figure 2.3 [6]. In this algorithm, paraffins are first accepted as feed and converted into carbenium ions via sequential dehydrogenation and protonation. The ions then undergo isomerization and cracking. The algorithm ensures that every new carbenium ion species undergoes isomerization, cracking

and deprotonation sequentially. The algorithm stops when no new ionic, olefinic or praffinic species is detected. This is established by having a separate flag for ions, olefins and paraffins. Whenever a flag turns 1, a new species is detected and it undergoes all the sequential reactions. When all three flags are zero, it indicates formation of no new species and the network algorthim terminates.

2.1.4. Network Generated Data

After complete network generation with the help of algorithm described in Section 2.1.3, a network of all elementary steps and species involved is obtained. The data in this network is extracted in the form of one long 2D matrix named as 'Reaction Network Data' and three 3D matrices named as 'Reactant Data', 'Product Data' and 'Olefin Product Data' respectively. Reaction Network Data is of dimensions (n x 6) and it contains information about all the reactions taking place in the network. Each row of this matrix contains information about one reaction and hence, the number of rows (n) of this matrix is equal to total number of reactions taking place in the network. In each row, first five elements indicate in boolean (0 or 1) if the reaction is methyl shift, PCP branching, cracking, hydride shift or protonation. For example, if a reaction is hydride shift, the first five elements of this row will be [0 0 0 1 0]. In case of cracking reaction, the sixth and last element of the row is non-zero and contains index of olefin product in stack named 'Olefin Product'. If a row represents protonation or isomerization reaction, this last element is 0. Reactant Data stack is of dimensions (7 x 7 x n) and it contains reactants participating in each of the reactions. Product Data stack is also of dimensions (7 x 7 x n) and consists of corresponding products of reaction. Olefin Product Data stack of dimensions (7 x 7 x n_{cr}) contains the olefin product of every cracking reaction whose index, is stored in last column of Reaction Network Data. Hence the number of matrices in this stack (n_{cr}) is equal to total number of cracking reactions taking place in the network. This data management system for reaction network is designed inhouse and is illustrated in detail in Figure 2.4.

The network generated data described above, is used to extract information about all isomerization and cracking reactions taking place in the network. The condensed form of this information is given in Table 2.3. The extracted information from Figure 2.4 is used to model net reaction rate equations for formation of each of the involved species. This reaction modelling is further elucidated in Section 2.3.1.

Table 2.3: Information extracted from network generated data for species and elementary reactions; the number of reactions are in 'n x 2' format as they encompass both forward and backward reactions. It is assumed that cracking only takes place in forward direction and there is no oligomerization of cracked products back into long chain alkanes. Hence cracking is not in 'n x 2' format.

Reaction Network Data	
Number of paraffins	12
Number of olefins	31
Number of carbenium ions	25
Protonation reactions	44 x 2
Deprotonation reactions	44 x 2
Hydride shifts	13 x 2
Methyl shifts	4 x 2
PCP branchings	29 x 2
Cracking reactions	5
Total number of elementary reactions	273

2.2. Kinetic coefficients via Single Event Micro-Kinetic model

In Table 2.3, it can be observed that the number of different elementary reactions is more than hundred. Hence, before modelling rate parameters and rate equations pertaining to all elementary reactions, it is important to define these rate parameters and reduce the num-

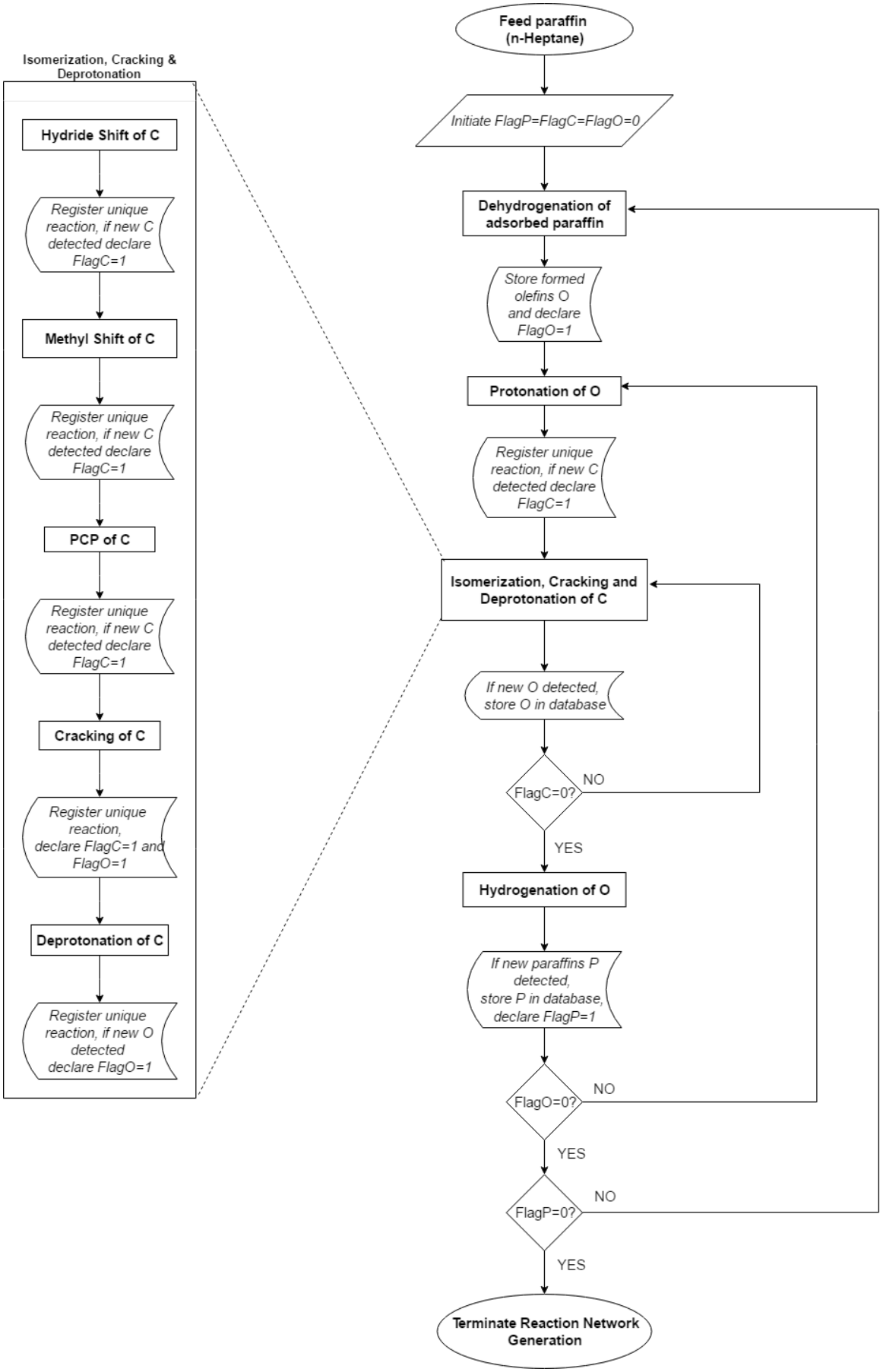

Figure 2.3: Computer Algorithm for Reaction Network Generation
FlagC: 0 if no new carbenium ion species formed; 1 if new carbenium ion species formed;
FlagO: 0 if no new olefin species formed; 1 if new olefin species formed,
FlagP: 0 if no new paraffin species formed; 1 if new paraffin species formed;
Register unique reaction: stores type of reaction, reactant BM and product BM

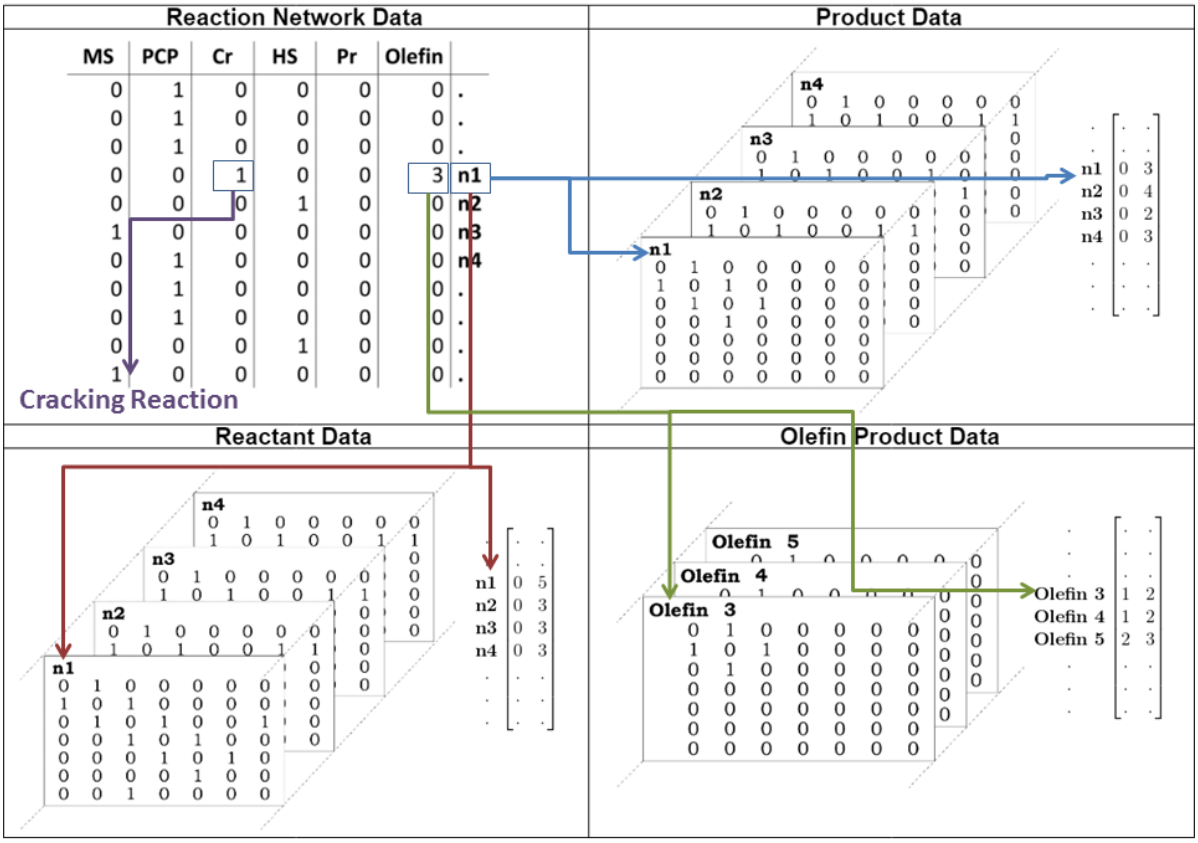

Figure 2.4: Data management system developed inhouse for storage of reactions, data is procured in the form of one long 2D matrix 'Reaction Network Data' and three 3D matrices namely, 'Reactant Data', 'Product Data' and 'Olefin Product Data'. Each row in 'Reaction Network Data' represents one reaction of type MS (methyl shift), PCP (PCP branching), Cr (cracking), HS (hydride shift) and Pr (Protonation). Index of each row represents index of reactant in 'Reactant Data' and index of product in 'Product Data'. For a cracking reaction, the additional olefin product is stored in 'Olefin Product Data' whose index is given in 'Olefin' column of 'Reaction Network Data'

ber of independent parameters as much as possible. This will help in deriving simpler rate equations with limited number of unknown parameters. In this section, firstly Transition State Theory is used to model rate constants for elementary steps [35]. Then, the number of independent rate constants are identified and reduced significantly in number by applying thermodynamic constraints.

2.2.1. Kinetic Rate Constant

According to Transition State Theory [35], the rate coefficient for an elementary step can be given as in Equation 2.2:

$$k = (\frac{k_b T}{h}) exp(\frac{\Delta S^o}{R}) exp(\frac{-\Delta H^o}{RT}) \tag{2.2}$$

The entropy of a species is given as summation of translation, rotational, vibrational and electronic contributions. The rotational contribution to entropy in itself consists of external and internal rotational terms as given in Equations 2.3 and 2.4 [11]. Here σ_{Ext} and σ_{Int} are external and internal symmetry numbers respectively.

$$S^{\circ}_{\text{ExtRot}} = \hat{S}^{\circ}_{\text{ExtRot}} - R\ln(\sigma_{\text{Ext}}) \tag{2.3}$$

$$S^{\circ}_{\text{IntRot}} = \hat{S}^{\circ}_{\text{IntRot}} - R\ln(\sigma_{\text{Int}}) \tag{2.4}$$

Table 2.4: Number of Single Events for Hydroisomerization and Hydrocracking Reactions. These expressions can be easily implemented in a computer algorithm [27]

Reaction Type	**Number of Single Events**
Protonation	1
Deprotonation	$n_{\alpha\mathrm{H}}$
Hydride Shift	$2n_{\alpha\mathrm{H}}$
Methyl Shift	$2n_{\alpha\mathrm{Me}}$
PCP Ring - α cleavage	$2n_{\beta\mathrm{H}}$
PCP Ring - β cleavage	2

When accounting for entropy of optically active compounds, an additional term $R\ln(2^n)$ is deducted from the entropy term. Here n is the number of chiral centres in the molecule. This term accounts for the loss of indistinguishability due to mixing of enantiomers. Hence the total rotational contribution of entropy is given by Equation 2.5.

$$S^{\circ}_{\mathrm{Rot}} = \hat{S}^{\circ}_{\mathrm{Rot}} - R\ln\left(\frac{\sigma_{\mathrm{Int}}\sigma_{\mathrm{Ext}}}{2^n}\right) \tag{2.5}$$

The term $R\ln(\frac{\sigma_{\mathrm{ext}}\sigma_{\mathrm{int}}}{2^n})$ is called as 'global symmetry number'. This term accounts for all the symmetry changes taking place in the reaction when the reactant converts into itermediate activated complex.

Ideally, symmetry number is calculated by counting the number indistinguishable structures obtained when the molecule is rotated about its terminal methyl rotors, external molecular axis and internal molecular axis [36]. This method requires structural identification of each reactant and activated complex involved in the reaction. It is not possible to calculate the symmetry number numerically when using structural identification techniques. This would require higher level molecular visualization programs and thus it is difficult to implement this method in a MATLAB code. In order to circumvent this inconvenient implementation, the ratio $(\frac{\sigma_{\mathrm{reactant}}}{\sigma_{\mathrm{activated\ complex}}}) = n_{\mathrm{e}}$ is taken into account. The ratio n_{e} corresponds to number of single events resulting in a particular same reaction. Number of single events can be equated to the ratio of statistical factors in the forward and reverse direction of the reaction [37]. For reactions involved in hydroisomerization of hydrocarbons, the ratio of statistical factors can be directly calculated using Table 2.4 [27]. This way the number of single events can be easily implemented in the computer algorithm.

The kinetic rate constant of any given reaction is thus given by Equation 2.6

$$k = \frac{\sigma^{\mathrm{R}}_{\mathrm{gl}}}{\sigma^{\neq}_{\mathrm{gl}}}\frac{k_{\mathrm{b}}T}{h}\exp\left(\frac{\Delta\hat{S}^{\circ}}{R}\right)\exp\left(\frac{-\Delta H^{\circ}}{RT}\right) = n_{\mathrm{e}}\hat{A}_{\mathrm{app}}\exp\left(\frac{-E_{\mathrm{a,app}}}{RT}\right) \tag{2.6}$$

$$n_{\mathrm{e}} = \frac{\sigma^{\mathrm{R}}_{\mathrm{gl}}}{\sigma^{\neq}_{\mathrm{gl}}} \tag{2.7}$$

Herein, n_{e} is the number of single events leading to the product as a result of reaction.

2.2.2. Independent Kinetic Parameters

As observed in Equation 2.6, a kinetic rate constant mainly comprises of two independent parts: Entropy contribution and Enthalpy contribution. These are the two unknown quantities to be found out for each type of reaction in order to get rate of formation of all components in reaction network. From Equation 2.6, it can be inferred that, rate equations for all the carbenium ions, olefins and paraffins will contain unknown kinetic coefficients as given in Table 2.5.

The entropy in Equation 2.6 comprises of translational, rotational, vibrational and electronic contributions [11]. For unimolecular reactions, the contribution of translational entropy term will be zero as the masses of reactant and activated complex are same. For all

Table 2.5: Number of unknown parameters pertaining to rate equations of carbenium ions, olefins and paraffins in reaction network prior to applying thermodynamic constraints and assumptions.

Reaction Type	**Unknown Parameters**
Protonation	44
Deprotonation	44
Hydride Shift	13
Methyl Shift	4
PCP Ring	29
Cracking	5
Total	**139**

isomerization reactions, once the contribution of symmetry in structures is factored out from rotational entropy terms, the remaining contribution by difference in moments of inertia of reactants and products can be considered same for all reactions belonging to a particular 'type' [1]. This is mainly due to the fact that in isomerization reactions, there are not much structural differences in reactants and activated complexes taking part in those reactions. A similar reasoning can be given for vibrational contributions. The number of electrons in reactant and activated complex are same, and hence electronic contribution can also be considered same for all reactions belonging to a given 'type'. Hence, $\Delta\hat{S}^{o}$ is a constant independent parameter for Protonation, Deprotonation, Hydride Shift, Methyl Shift and PCP decomposition reactions.

The activation energy term in Equation 2.6 depends on changes in energy levels of reactant and product carbenium ions. It is assumed that the energy level of reactant and product only depends on the secondary/tertiary nature of carbenium ions. This means, only the contribution of α carbon atoms with respect to positive charge is considered for the change in energy levels of reactants and activate complexes.

On the basis of above asumptions, the number of independent parameters can be further reduced according to simplifications for each of type of reaction as follows:

Protonation

The kinetic rate constant of protonation is independent of olefin participating in reaction. This assumption is valid due to similarities in the structure of reacting olefin and corresponding activated complex [6]. The latter differs from the former only by its 2D planar structure. With the assumption that change in energy and entropy only depends on type of carbenium ion (secondary or tertiary) and not on chain length, branches etc., it can be inferred that kinetic coefficient for protonation is a function of only the resulting carbenium ion [11, 27]. Hence $k_{\mathrm{pr}}(\mathrm{s})$ and $k_{\mathrm{pr}}(\mathrm{t})$ are the only independent kinetic parameters. This reduces number of independent rate constants for protonation from 44 to 2.

Deprotonation

The kinetic rate constant for any deprotonation reaction can be expressed in terms of kinetic rate constant of deprotonation of a reference olefin and equilibrium constant of isomerization between reference olefin and the olefin participating in deprotonation reaction [6]. This co-relation is derived as follows:

Two olefin isomers O_1 and $\mathrm{O}_{\mathrm{ref}}$ can be related to each other via reactions in Scheme 2.12:

$$\mathrm{O}_1 + \mathrm{H}^+ \quad \underset{k_{\mathrm{de}}(\mathrm{s};\mathrm{O}_1)}{\overset{k_{\mathrm{pr}}(\mathrm{s})}{\rightleftharpoons}} \quad \mathrm{R}_1^+ \quad \underset{k_{\mathrm{pr}}(\mathrm{s})}{\overset{k_{\mathrm{de}}(\mathrm{s};\mathrm{O}_{\mathrm{ref}})}{\rightleftharpoons}} \quad \mathrm{O}_{\mathrm{ref}} + \mathrm{H}^+$$

Scheme 2.12: Reaction Scheme relating O_1 and O_{ref}

If carbenium ion R_1^+ is a secondary ion, relation in Equation 2.8 can be given for equilibrium constant for isomerization between O_1 and $\mathrm{O}_{\mathrm{ref}}$.

[1] 'type' here means: protonation, deprotonation and isomerization reactions

$$K_{\mathrm{iso}}(\mathrm{O_{ref}} \leftrightharpoons \mathrm{O_1}) = \frac{k_{\mathrm{pr}}(\mathrm{s})}{k_{\mathrm{de}}(\mathrm{s};\mathrm{O_1})} \frac{k_{\mathrm{de}}(\mathrm{s};\mathrm{O_{ref}})}{k_{\mathrm{pr}}(\mathrm{s})} \tag{2.8}$$

Thus, for a given carbenium ion type and given carbon number (C_7, C_3, C_4 for present work), Equation 2.9 gives its deprotonation kinetic rate constant where z represents protonation into either secondary ion (s) or tertiary ion (t).

$$k_{\mathrm{de}}(z;\mathrm{O_1}) = k_{\mathrm{de}}(z;\mathrm{O_{ref}}) * K_{\mathrm{iso}}(\mathrm{O_{ref}} \leftrightharpoons \mathrm{O_1}) \tag{2.9}$$

Equation 2.9 reduces the number of independent rate constants for deprotonation from 44 to 4 (2 for C_7, 1 for C_3, 1 for C_4). The equilibrium constant $K_{\mathrm{iso}}(\mathrm{O_{ref}} \leftrightharpoons \mathrm{O_1})$ can be calculated using relations involving standard thermodynamic state functions as given in Equations 2.10 and 2.11.

$$K_{\mathrm{iso}}(\mathrm{O_{ref}} \leftrightharpoons \mathrm{O_1}) = \exp\left(\frac{-\Delta G^{\mathrm{o}}_{\mathrm{iso}}}{RT}\right) \tag{2.10}$$

$$\Delta G^{\mathrm{o}}_{\mathrm{iso}} = \Delta H^{\mathrm{o}}_{\mathrm{iso}} - T\Delta S^{\mathrm{o}}_{\mathrm{iso}} \tag{2.11}$$

The standard change in gibbs energy $\Delta G^{\mathrm{o}}_{\mathrm{iso}}$ for the reaction was obtained as difference in standard gibbs energy of formation of reactants and products. These values were obtained from literature using Benson's group contribution method [38]. The data was obtained at the operating temperature of reactions.

Isomerization

The rate coefficient for isomerization depends only on type of carbenium ions involved and not on their corresponding chain lengths and branches [6]. With this assumption , only for 4 independent kinetic parameters ((s;s), (s;t), (t;s) and (t;t)) are required for each type of isomerization reaction. Using thermodynamic analysis, Equation 2.12 was derived for all the required isomerization reactions of carbenium ions [27].

$$\frac{k_{\mathrm{iso}}(\mathrm{t;s})}{k_{\mathrm{iso}}(\mathrm{s;t})} = \frac{k_{\mathrm{pr}}(\mathrm{s})}{k_{\mathrm{pr}}(\mathrm{t})} * \frac{k_{\mathrm{de}}(\mathrm{t};\mathrm{O_{ref}})}{k_{\mathrm{de}}(\mathrm{s};\mathrm{O_{ref}})} \tag{2.12}$$

This reduces the number of independent rate parameters for each type of isomerization from 4 to 3. In Equation 2.12, rate constants of deprotonation of reference olefin is involved. If the ratio $\frac{k_{\mathrm{de}}(\mathrm{t;O_{ref}})}{k_{\mathrm{de}}(\mathrm{s;O_{ref}})}$ is not same for olefins of different carbon numbers, the ratio $\frac{k_{\mathrm{iso}}(\mathrm{t;s})}{k_{\mathrm{iso}}(\mathrm{s;t})}$ will change according to carbon number of reference olefin. To avoid this disparity, the ratio $\frac{k_{\mathrm{de}}(\mathrm{t;O_{ref}})}{k_{\mathrm{de}}(\mathrm{s;O_{ref}})}$ should be equal across all carbon numbers as given by Equation 2.13.

$$\frac{k_{\mathrm{de}}(\mathrm{t};\mathrm{O_{ref7}})}{k_{\mathrm{de}}(\mathrm{s};\mathrm{O_{ref7}})} = \frac{k_{\mathrm{de}}(\mathrm{t};\mathrm{O_{ref4}})}{k_{\mathrm{de}}(\mathrm{s};\mathrm{O_{ref4}})} = \frac{k_{\mathrm{de}}(\mathrm{t};\mathrm{O_{ref3}})}{k_{\mathrm{de}}(\mathrm{s};\mathrm{O_{ref3}})} \tag{2.13}$$

However, as a tertiary bonded alkene isomer of propene does not exist, $C_3H_7^+$ ions do not require deprotonation rate constant of tertiary ions ($k_{\mathrm{de}}(\mathrm{t};\mathrm{O_{ref3}})$). Hence, the equality in Equation 2.13 gives rise to estimation of rate constant for deprotonation of reference olefin of C_4H_8 as follows:

$$k_{\mathrm{de}}(\mathrm{t};\mathrm{O_4}) = k_{\mathrm{de}}(\mathrm{s};\mathrm{O_4}) * \frac{k_{\mathrm{de}}(\mathrm{t};\mathrm{O_7})}{k_{\mathrm{de}}(\mathrm{s};\mathrm{O_7})} \tag{2.14}$$

Final Independent Parameters

After applying all the above given simplifications, number of independent kinetic parameters are reduced from 139 to 19. All the required independent parameters to be calculated for optimizing fitting of model with experimental data are in Table 2.6

Table 2.6: Independent rate constants for all reactions in reaction network after application of thermodynamic constraints and assumptions. Here, for rate constants of cracking reactions, B1, B2 and C refer to types of cracking reactions and k_{cr} of type (R_1; R_{cr1}, O_{cr1}) refers to cracking of carbenium ion R_1 into ion R_{cr1} and olefin O_{cr1}.Identities of each of the species in this table are given in the Appendix Table A.1.

Reaction	**Independent Parameters**	
	Parameter	Type
Protonation	k_{pr}	s
	k_{pr}	t
Hydride Shift	k_{hs}	s;s
	k_{hs}	s;t
	k_{hs}	t;t
Methyl Shift	k_{ms}	s;s
	k_{ms}	s;t
PCP	k_{pcp}	s;s
	k_{pcp}	s;t
	k_{pcp}	t;t
Deprotonation	k_{de}	s;O_{ref7}
	k_{de}	t;O_{ref7}
	k_{de}	s;O_{ref4}
	k_{de}	s;O_{ref3}
Cracking	k_{cr}B2	R_1;R_{cr1},O_{cr1}
	k_{cr}C	R_2;R_{cr2},O_{cr2}
	k_{cr}C	R_3;R_{cr3},O_{cr3}
	k_{cr}B1	R_4;R_{cr4},O_{cr4}
	k_{cr}C	R_5;R_{cr5},O_{cr5}

2.3. Rate Equations and Reactor Model

In this section, firstly, rate equation for each step involved in hydroisomerization and hydrocracking n-Heptane is obtained using independent rate parameters, which derived in Section 2.2.2 and summarized in Table 2.6, to derive production rates for each paraffin species in the network. These steps include elementary reactions described in Section 2.1.2 as well as adsorption, dehydrogenation, hydrogenation and desorption. These steps are sequentially described along with corresponding reactions in Table 2.7. In the second half of this section, rate equations for net production of product paraffins are used to derive an overall conversion model across the length of reactor.

2.3.1. Development of Rate Equations

As the paraffins (P_i) enter catalyst in gaseous phase, they are physisorbed into pores of catalyst ($q_{s,i}$). This physisorbtion is modelled by means of Langmuir Isotherms given by Equation 2.15. In this equation, i stands for individual paraffin species, p_i for partial pressure of paraffin species and q_{si} for physisorbed paraffin species. In present work, the paraffin entering catalyst at the inlet of reactor is n-Heptane (C_7H_{16}).

$$q_{s,i} = \frac{q_{sat,i} * b_i * p_i}{(1 + \sum_{i=1}^{10}(b_i * p_i))} \tag{2.15}$$

The physisorbed paraffins ($P_{i,adsorbed}$) undergo dehydrogenation at metal sites in catalyst.

$$P_{i,adsorbed} \underset{k_h(O_{ij};i)}{\overset{k_{dh}(i;O_{ij})}{\rightleftharpoons}} O_{ij} + H_2$$

Scheme 2.13: Dehydrogenation and hydrogenation reaction

The equilibrium constant $K_{eq} = \frac{k_{dh}(i;O_{ij})}{k_h(O_{ij};i)}$ for this reaction is calculated using thermodynamic state functions. The thermodynamic properties of Alkenes are obtained using Ben-

Table 2.7: All the steps that are involved in hydroisomerization and hydrocracking of n-heptane in bifunctional catalyst. All these steps are implemented in the reactor network. [39]

Reaction	Description
$P_{gas} + zeolite \overset{Eq}{\rightleftharpoons} P_{adsorbed}$	Physisorption of incoming paraffin (P_{gas}) into pores of catalyst
$P_{adsorbed} \overset{Eq}{\rightleftharpoons} O + H_2$	Dehydrogenation of adsorbed paraffins ($P_{adsorbed}$) into olefins (O) at metal sites of catalyst
$O + H^+ \overset{k_{pr}(z)}{\rightleftharpoons} R_k^+$	Protonation of olefins and deprotonation of carbenium ions (R_k^+) at acid sites
$R_k^+ \underset{k_{iso,b}((m;k))}{\overset{k_{iso,f}(k;m)}{\rightleftharpoons}} R_m^+$	Isomerization reactions (hydride shift, methyl shift, PCP branching) of carbenium ions (R_k^+, R_m^+) at acid sites
$R_k^+ \overset{k_{cr}(k;p,O')}{\rightarrow} R_p^+ + O'$	Cracking of carbenium ions (R_k^+) on acid sites into product carbenium ions (R_p^+) and olefins (O')
$R^+ \overset{k_{de}(z;O'')}{\rightleftharpoons} O'' + H^+$	Deprotonation of all carbenium ions R^+ (isomerized and cracked) into olefins (O'')
$O'' + H_2 \overset{Eq}{\rightleftharpoons} P'_{adsorbed}$	Hydrogenation of all olefins into paraffins ($P'_{adsorbed}$) at metal sites
$P'_{adsorbed} \overset{Eq}{\rightleftharpoons} P'_{gas} + zeolite$	Desorption of all paraffins from metal sites

son's group contribution method [38].

The concentration of olefins ($C_{O_{ij}}$) can be obtained using K_{eq}, concentration of physisorbed olefins ($C_{P_{i,adsorbed}}$) and partial pressure of hydrogen (p_{H_2}) as in Equation 2.16.

$$K_{eq} = \frac{C_{O_{ij}} * p_{H_2}}{C_{P_{i,adsorbed}}}$$

$$C_{O_{ij}} = \frac{K_{eq} * C_{P_{i,adsorbed}}}{p_{H_2}} \tag{2.16}$$

The 31 species of formed olefins are protonated into 25 different species of carbenium ions at acid sites of catalysts. Each olefin (O_{ij}) can form 2 different or 1 (if one of the ions is primary in nature) carbenium ion species. Similarly 2 different carbenium ions (R_k^+, R_l^+) can deprotonate into an identical olefin.

$$O_{ij} + H^+ \underset{k_{de}(z;O_{ij})}{\overset{k_{pr}(z)}{\rightleftharpoons}} \begin{cases} R_k^+ \\ R_l^+ \end{cases}$$

Scheme 2.14: Protonation and deprotonation Reaction

Thus formed carbenium ions then undergo isomerization (Schemes 2.15, 2.16 and 2.17), cracking (Scheme 2.18), deprotonation and hydrogenation reactions to ultimately result in new species of carbenium ions, olefins and paraffins.

$$R_k^+ \underset{k_{hs}(m;k)}{\overset{k_{hs}(k;m)}{\rightleftharpoons}} R_m^+$$

Scheme 2.15: Hydride shift reaction

As a result of all reactions, the net rate of formation of a particular carbenium ion R_k^+ can be given by expression in Equation 2.17.

$$R_k^+ \underset{k_{ms}(n;k)}{\overset{k_{ms}(k;n)}{\rightleftharpoons}} R_n^+$$

Scheme 2.16: Methyl shift reaction

$$R_k^+ \underset{k_{pcp}(o;k)}{\overset{k_{pcp}(k;o)}{\rightleftharpoons}} R_o^+$$

Scheme 2.17: PCP branching reaction

$$R_k^+ \xrightarrow{k_{cr}(k;p,O_{qr})} R_p^+ + O_{qr}$$

Scheme 2.18: Cracking reaction

$$R_{R_k^+} = \sum_O k_{pr}(z) C_O C_{H^+} + \sum_m k_{hs}(m;k) C_{R_m^+} + \sum_n k_{ms}(n;k) C_{R_n^+} + \sum_o k_{pcp}(o;k) C_{R_o^+} + \sum_s k_{cr}(s;k,O) - \left(\sum_O k_{de}(k;O) + \sum_t k_{hs}(k;t) + \sum_u k_{ms}(k;u) + \sum_v k_{pcp}(k;v) C_{R_v^+} + \sum_p k_{cr}(k;p,O_{qr}) \right) C_{R_k^+} \quad (2.17)$$

The concentration of free acid sites in catalyst (C_{H^+}) can be given by substraction of occupied acid sites by carbenium ions ($C_{R_i^+}$)from the total concentration of active acid sites (C_t) in catalyst as given in Equation 2.18. The total concentration of acid sites is calculated using catalyst specific information for BEA from online zeolites structure database [40].

$$C_{H^+} = C_t - \sum_{i=1}^{25} C_{R_i^+} \quad (2.18)$$

Psuedo steady state approximation is applied on the net rate of formation of all carbenium ions to yield Equation 2.19. This is a set of 25 simultaneous linear equations encompassing all carbenium ion species in the system. These equations can be straightforwardly solved to yield concentrations of all 25 carbenium ion species.

$$\sum_{i=1}^{25} R_{R_i^+} = 0 \quad (2.19)$$

As represented in Scheme 2.19, paraffins are formed by dehydrogenation of corresponding olefins. Thus the rate of formation of a particular paraffin is given by Equation 2.20.

$$R_{P_i} = \sum_j \left(k_h(O_{ij};i) C_{O_{ij}} p_{H_2} - k_{dh}(i;O_{ij}) C_{P_i} \right) \quad (2.20)$$

As given in Schemes 2.14, 2.18 and 2.19, an olefin O_{ij} is involved in protonation, deprotonation, cracking, hydrogenation and dehydrogenation reactions. Hence the rate of formation of an olefin is given by Equation 2.21.

$$R_{O_{ij}} = k_{dh}(i;O_{ij}) C_{P_i} - k_h(O_{ij};i) C_{O_{ij}} p_{H_2} + k_{de}(z_1;O_{ij}) C_{R_k^+} + k_{de}(z_2;O_{ij}) C_{R_l^+} - \left(k_{pr}(z_1) + k_{pr}(z_2) \right) C_{O_{ij}} C_{H^+} + k_{cr}(w;x,O_{ij}) C_{R_w^+} \quad (2.21)$$

Using steady state approximation for olefins gives Equation 2.22 which ultimately leads to Equation 2.23.

$$R_{O_{ij}} = 0 \quad (2.22)$$

$$O_{ij} + H_2 \underset{k_{dh}(i;O_{ij})}{\overset{k_h(O_{ij};i)}{\rightleftharpoons}} P_i$$

Scheme 2.19: Hydrogenation and dehydrogenation of paraffins

$$k_h(O_{ij};i)C_{O_{ij}}p_{H_2} - k_{dh}(i;O_{ij})C_{P_i} = k_{de}(z_1;O_{ij})C_{R_k^+} + k_{de}(z_2;O_{ij})C_{R_l^+} - \left(k_{pr}(z_1) + k_{pr}(z_2)\right)C_{O_{ij}}C_{H^+} + k_{cr}(w;x,O_{ij})C_{R_w^+} \quad (2.23)$$

The right hand side of Equation 2.23 is the net rate of formation of Paraffin P_i by dehydrogenation of Olefin O_{ij}. The hydrogenation of olefins and dehydrogenation of paraffins are the only reactions in which paraffins participate. Hence net rate of formation of paraffins is given by Equation 2.24.

$$R_{P_i} = \sum_j \left(k_{de}(z_1;O_{ij})C_{R_k^+} + k_{de}(z_2;O_{ij})C_{R_l^+} - \left(k_{pr}(z_1) + k_{pr}(z_2)\right)C_{O_{ij}}C_{H^+} + k_{cr}(w;x,O_{ij})C_{R_w^+}\right) \quad (2.24)$$

2.3.2. Reactor Model

Equation 2.24 gives the net rate of formation of paraffins as a result of series of hydrogenation, dehydrogenation, isomerization and cracking reactions undergone by each of 12 paraffin species. The concentration of olefin species ($C_{O_{ij}}$) required in expression 2.24 are obtained from Equation 2.16 and the concentration of carbenium ion species are extracted by solving Equation 2.19.

The overall production of a particular paraffin P_i at a given length z inside the reactor for non-steady state is given by Equation 2.25. Here R_{P_i} is the net rate of production of paraffin P_i.

$$\frac{1}{RT}\frac{dp_i}{dt} = \frac{-u}{RT}\frac{dp_i}{dz} + \rho_{cat}\frac{1-\epsilon}{\epsilon}R_{P_i} \quad (2.25)$$

For a reactor in steady state, the disctribution of partial pressure of paraffin i along the length of reactor in z-direction is given by Equation 2.26

$$\frac{u}{RT}\frac{dp_i}{dz} = \rho_{cat}\frac{1-\epsilon}{\epsilon}R_{P_i} \quad (2.26)$$

The production term R_{P_i} here can be given by Equation 2.24.

For a reactor of length L divided into total of n_t nodes, the differential pressure dp_i across n^{th} node is given by Equation 2.27 and the differential length dz is given by Equation 2.28.

$$dp_i = \Delta p_i = p_i^{n+1} - p_i^n \quad (2.27)$$

$$dz = \frac{L}{n_t} \quad (2.28)$$

Thus the partial pressure of paraffin species i at the end of n^{th} node, taking the partial pressure of the same species at the end of $(n\text{-}1)^{th}$ node as input, is given by Equation 2.29.

$$p_i^{n+1} = p_i^n + \frac{L}{un_t}\rho_{cat}RT\frac{1-\epsilon}{\epsilon}R_{P_i}^n \quad (2.29)$$

All of thus far derived species concentrations and rate expressions were implemented in MATLAB codes and these codes were run through a series of Genetic Algorithm optimization iterations to obtain the independent kinetic parameters described in Table 2.6. Detailed explanation and results of optimization program are described in Chapter 3.

3

Simulation Details

This chapter gives information on inlet conditions and details of simulations performed to carry out this study.

3.1. Inlet Conditions

The inlet pressure of n-Heptane into the reactor is 1.19×10^5 Pa. Pressure of hydrogen gas at inlet of reactor is 2.98×10^6 Pa. Since there is 25 times more supply of hydrogen gas than n-Heptane, consumption of hydrogen is negligible and it is assumed to be constant throughout the reactor. An operating temperature range of 246°C - 271°C is used for carrying out simulations for a good visualization and grasping of product distributions. Simulations are carried at temperatures 246°C (519K), 258°C (531K), and 271°C (544K). For these temperatures conversion of n-Heptane is observed approximately between 10% and 60%.

3.2. Simulation details of Genetic Algorithm and optimization criteria

Genetic Algorithm (GA) in optimization is used for finding minima of highly non-linear problems [41]. This optimization algorithm is based on bio-inspired process of natural selection in evolutionary algorithms. Every iteration step in GA is called as 'generation'. At each generation, instead of single guess values, a set of guess values called as 'population' is generated. The number of guess values in population is given by specifying the 'population size'. At first generation, a population of random guesses is generated and fitting of each guess is checked. The guesses with good fit are as it is passed on to the next iteration. They also undergo mutation and crossover rules to give new set of values towards better fitting. Hence, values with best fit, mutated and crossover values and randomly generated guess values form a set of population for next generation [42]. MATLAB computing environment has in-built function for GA and it is implemented in this study with following set values and criteria:

Object Function: Estimations of parameters are obtained by minimizing objective function in Equation 3.1

$$S = \sum_{i=1}^{l} \sum_{j=1}^{s} \sqrt{w_S (E_{ij} - M_{ij})^2} \tag{3.1}$$

Here l is the number of discrete points across the length of reactor where experimental concentrations were measured, s is the number of paraffins, w_S is a scaling factor and it is 10^2 for dimethylpentanes and 1 for others, E_{ij} is experimental concentration of paraffin and M_{ij} is concentration of paraffin obtained from the model. Experimental results were obtained at five discrete points ($\frac{1}{3}l$, $\frac{1}{2}l$, $\frac{2}{3}l$, $\frac{5}{6}l$ and l) across the length of reactor. The concentrations of

dimethylpentanes are very low and hence a scaling factor of $w_S = 10^2$ is used to make their contribution to the object function significant.

Population size: Taking a large population size ensures that enough number of distinct guess values are taken into consideration and the solution is not stuck in a local minima. After initial runs, it was observed that a population size of 5×10^3 gave best possible fits and this value was thus used to carry out rest of the study.

3.3. Simulation details for single node and whole reactor

The simulation is divided into three main parts:

1. Reaction network code on single node
2. Whole reactor code
3. Main code

Reaction network code on single node: This code simulates the reactions taking place at each node in reactor. The model developed in Chapter 2 which is based on SEMK approach and is developed for hydroisomerization and hydrocracking of n-heptane is incorporated in this code. Paraffins entering at beginning of node undergo adsorption, dehydrogenation, protonation, isomerization and cracking reactions inside the node and resulting concentration of paraffins at the output of node are computed in this code.

Whole reactor code: This code compiles the input and output of paraffins at all nodes in the reactor. At each node, the function for reaction network at single node is called and the output concentrations of paraffins are recorded.

Main code: This code computes the object function for concentrations across the length of reactor for a particular temperature. The function for genetic algorithm is called and object function is computed for each of the guess values.

Simulation flow: An ensemble of the three codes described above are used to perform the fitting of model into experimental data and the rate constants for the best fit are are computed. The flow of control between these codes is described in Figure 3.1.

3.4. Additional changes

After initial simulations runs, it was obeserved that certain changes were needed to accurately fit the model to experimental results at the given reaction conditions. The two changes made to the simulation were:

- Negligible concentrations of 3-Ethylpentane and 2,2,3-Trimethylbutane were observed in model fitting and zero concentration was observed in experimental results. Hence carbenium ion, olefins and reactions related to any of these two species were removed from the reaction etwork.
- An excessive amount of 3,3-Dimethylpentane was observed in the model as compared to experimental results. Also in the experimental results, it was observed that every isomer of heptane present in the system underwent cracking. Hence a psuedo cracking reaction of type B1 for conversion of 3,3-Dimethylpentane-2+ into 2-Methylpropane-2+ and Propene was assumed to achieve a better fitting of model.

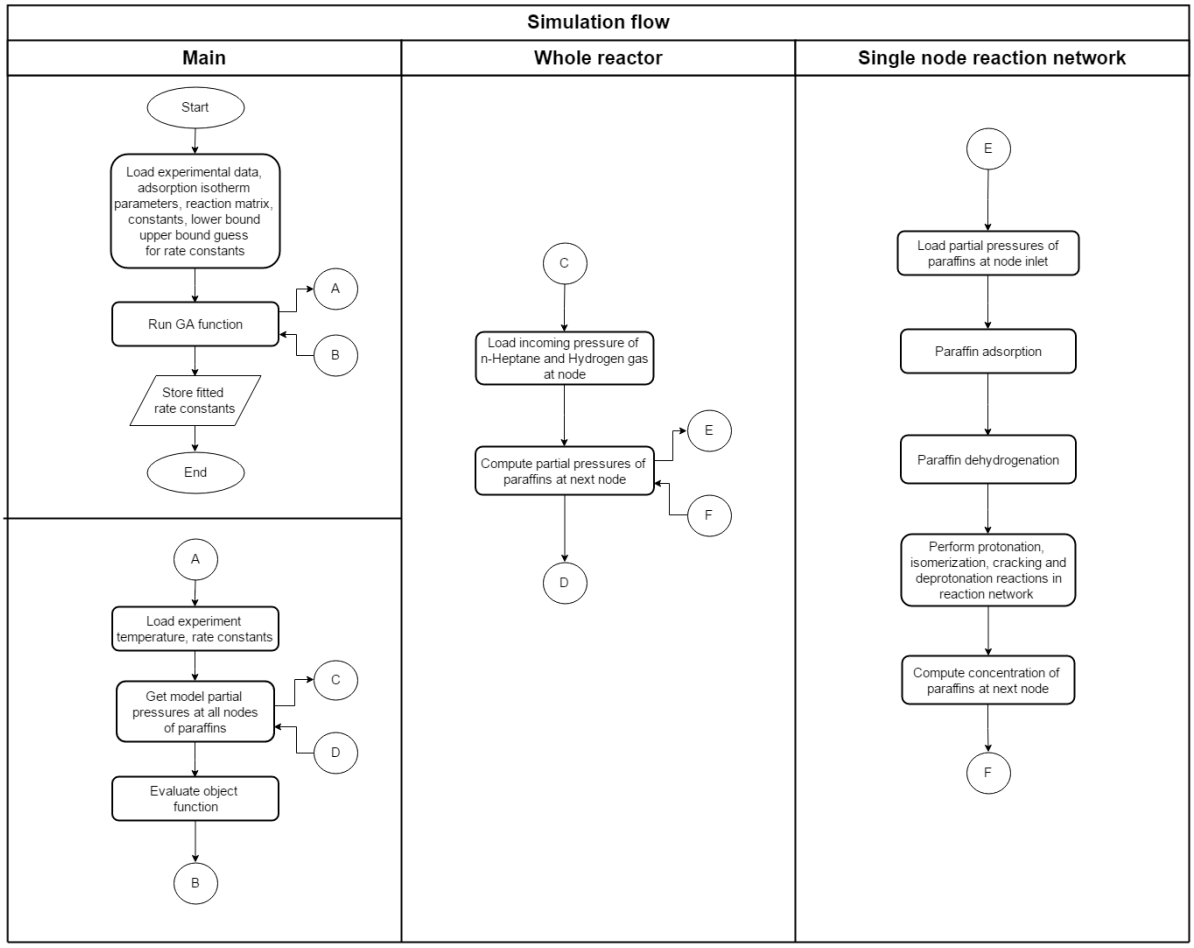

Figure 3.1: Flow of control in the overall simulation. The simulation can be divided into three segments: Main, Whole reactor and Single node reaction network. The Single node reaction network code implements all the elemenary steps taking place at each node of reactor. The Whole reactor code implements continuous flow of components across the reactor in steady state. The overall fitting of model to experimental results is performed in the Main code.

3.5. Validation of Simulation

The validation of simulation was performed in two parts. First, the code for reaction network generation was validated by comparing reaction data obtained for hydroisomerization and hydrocracking of n-Octane with literature. Next the reactor network code is validated by checking the mass balance across the reactor.

3.5.1. Reaction network validation

The code developed for computer generation of reactor network is based on approach deveoped by Baltanas et al. [30]. The code developed for this work is created for hydroisomerization and hydrocracking of n-Octane. Svoboda et al. developed a similar SEMK model for hydroisomerization and hydrocracking of n-Octane [31]. In the reaction network generated for this model by Svoboda et al., 22 paraffins are observed. Modifications were made to the present model in order to generate reaction network for n-Octane hydroisomerization and hydrocracking. The number of paraffins observed in reaction network generated after running the simulation code developed for present work are 22 as is also observed by Svoboda et al. The time required for entire reaction network generation in case of n-Octane was 15 times higher than that for n-Heptane. This is expected as the number of isomers and cracked products in hydroisomerization and hydrocracking of n-Octane is twice that of n-Heptane.

3.5.2. Balance of mass across reactor

In the simulation results, mass balance is validated for flow of components across the reactor length by checking the flow of mass at five lengths across the reactor. Mass balance across the reactor is necessary to ensure that the reactions at steady state are balanced and there is not build up or loss of mass at any point in the reactor. In this work, balance of mass flow across the reactor was ensured by checking the mass of total hydrocarbons at different lengths across the reactor. The overall reaction for hydrocracking of heptanes is as given in Scheme 3.1.

$$C_7H_{16} + H_2 \longrightarrow C_3H_8 + C_4H_{10}$$

Scheme 3.1: Overall cracking reaction

According to Scheme 3.1, concentrations of heptane, butane and propane species are correlated to each other by Equations 3.2, 3.3 and 3.4. Here C_7, C_4 and C_3 are sum of concentrations of all isomers of heptane, butane and propane.

$$-\frac{dC_7}{dt} = \frac{dC_4}{dt} = \frac{dC_3}{dt} \tag{3.2}$$

$$\frac{dC_7}{dt} + \frac{dC_3}{dt} = 0 \tag{3.3}$$

$$\frac{dC_7}{dt} + \frac{dC_4}{dt} = 0 \tag{3.4}$$

According to Equation 2.29 derived in Section 2.3.2, the partial pressure of each paraffin species at each reactor node n+1 is given as function of partial pressure at previous node n as follows:

$$p_i^{n+1} = p_i^n + \frac{L}{un_t}\rho_{cat}RT\frac{1-\epsilon}{\epsilon}R_{P_i}^n$$

The factor $K = \frac{L}{un_t}\rho_{cat}RT\frac{1-\epsilon}{\epsilon}$ is same for all paraffin species. Equation 2.29 when summed over all heptane and butane isomers results in Equation 3.5.

$$\sum_{C_7\ \&\ C_4} p_i^{n+1} = \sum_{C_7\ \&\ C_4} p_i^n + K \sum_{C_7\ \&\ C_4} R_{P_i}^n \tag{3.5}$$

From Equation 3.4 it is inferred that the last term in Equation 3.5 is equal to zero (Equation 3.6).

$$\sum_{C_7\ \&\ C_4} R_{P_i}^n = 0 \tag{3.6}$$

Hence Equations 3.7 and 3.8 are derived for partial pressures of heptane, butane and propane species. In order to investigate the mass balance for present model, partial pressures of heptane, butane and propane species were examined at six nodes across the length of reactor (0, $\frac{1}{3}l$, $\frac{1}{2}l$, $\frac{2}{3}l$, $\frac{5}{6}l$ and l, here l is the length of reactor). The results for reaction temperature of 569K are summarized in Table 3.1. Detail summary of partial pressures of each species at each node in the reactor for all reaction temperatures can be found in appendix***.

$$\sum_{C_7\ \&\ C_4} p_i^{n+1} = \sum_{C_7\ \&\ C_4} p_i^n \tag{3.7}$$

$$\sum_{C_7\ \&\ C_3} p_i^{n+1} = \sum_{C_7\ \&\ C_3} p_i^n \tag{3.8}$$

A pressure profile of heptane isomers, butane isomers and propane species is presented in Figure 3.2. It can be seen in Table 3.1 and Figure 3.2 that as total pressure of heptanes

Table 3.1: Partial pressure profile of heptanes, butanes and propane across the reactor. The last two columns indicate constant flow of total mass in the reactor.

Dimensionless length across reactor	Partial pressure of species (Pa)				
	Total heptane (C_7)	Total butane (C_4)	Total propane (C_3)	Total hydrocarbons ($C_7 + C_3$)	Total hydrocarbons ($C_7 + C_4$)
0 (reactor inlet)	1.2E+05	0.0E+00	0.0E+00	**1.2E+05**	**1.2E+05**
0.33	1.0E+05	1.5E+04	1.5E+04	**1.2E+05**	**1.2E+05**
0.5	1.0E+05	1.9E+04	1.9E+04	**1.2E+05**	**1.2E+05**
0.67	9.7E+04	2.2E+04	2.2E+04	**1.2E+05**	**1.2E+05**
0.83	9.4E+04	2.5E+04	2.5E+04	**1.2E+05**	**1.2E+05**
1 (reactor outlet)	9.2E+04	2.7E+04	2.7E+04	**1.2E+05**	**1.2E+05**

gradually decreases across the length of reactor, butane and propane increases. Total partial pressure of butane and propane is same at each point of reactor. This is in line with overall reaction given in Scheme 3.1. The sum of partial pressures of heptanes and butanes as well as heptanes and propane remains constant. The results observed in Table 3.1 and Figure 3.2 confirm that there is no build up or loss of mass at any point and the mass is balanced across the length of reactor.

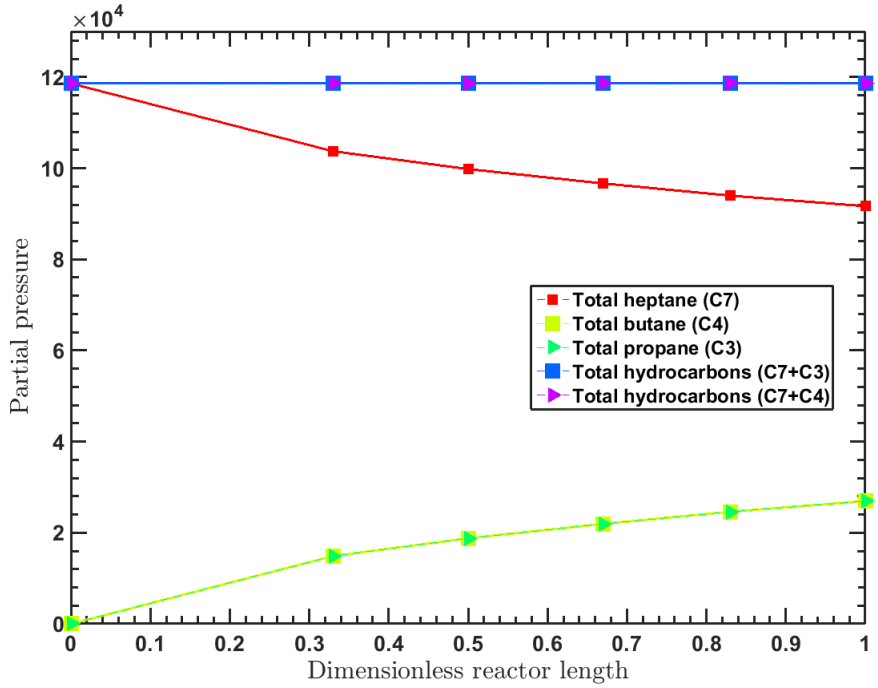

Figure 3.2: Partial pressure profile of heptanes, butanes and propane across the reactor at reaction temperature of 569K. The constant profile of total hydrocarbons ($C_7 + C_3$ and $C_7 + C_4$) indicates mass balance in the reactor.

4

Results and Discussions

This chapter reviews the results obtained in this work. The results are divided in two parts. In the first part, concentrations of all components are analyzed across the length of reactor and compared with experimental results. In the second part of this chapter, the computed rate constants as a result of simulations are analyzed to compare trends with literature.

4.1. Product distributions

In order to achieve better comprehension of isomerization and cracking, it is important to analyze the product distribution at different reactor lengths and temperatures. In this section, overall conversion and product distribution predicted by the model fitted to experimental data is examined. First, overall fitting of model with experiments is analyzed by looking at parity plots. Next, the product distribution is analyzed and compared with literature.

4.1.1. Parity

In present work, plots are created for concentrations at dimensionless reactor lengths of $\frac{1}{3}$, $\frac{1}{2}$, $\frac{2}{3}$, $\frac{5}{6}$ and 1 for each of the paraffins at reaction temperatures of 246°C (519K), 258°C (531K) and 271°C (544K). The plots are presented in Figures 4.1a, 4.1b and 4.1c. In these figures, it is observed that conversion of n-Heptane increases as reaction temperature rises. About 54% conversion of n-Heptane is observed at temperature 544K. Among the isomers of heptane, monobranched isomers are observed to be greater in concentration than any other species at all temperatures. The dibranched isomers are observed to be less than 0.1 mole fraction at all temperatures. Cracking is observed to be almost negligible at 519K and 531K. A detail analysis of distribution of each isomer and cracked product is performed in Section 4.1.2. Another observation in Figure 4.1 is the changes in R-squared values for different temperature. R-squared values give a measure of goodness of fitting of model to experimental values [43]. An R-squared value close to 100% indicates a good fitting of model to experimental data. In Figure 4.1, it can be observed that the fitting is good at low temperatures (519K and 531K) with R-squared values of almost 100%. At 544K, the R-squared value is slightly lower as compared to those at other temperatures. Although the high R-sqaured values for low temperatures can be attributed to low values of mole fractions of dibranched and cracked products, the good fitting is also indicative of accurate model values of conversion of n-Heptane at low reaction temperatures.

4.1.2. Product distribution of each component at all temperatures

A product wise distribution at all temperatures is presented in Figures 4.2, 4.3, 4.4 and 4.5. Distribution of n-Heptane at various reaction temperatures is presented in Figure 4.2. It is observed that overal conversion of n-Heptane increases as reaction temperature rises. An analysis of distribution of each of the products formed as a result of the conversion is presented in ensuing paragraphs.

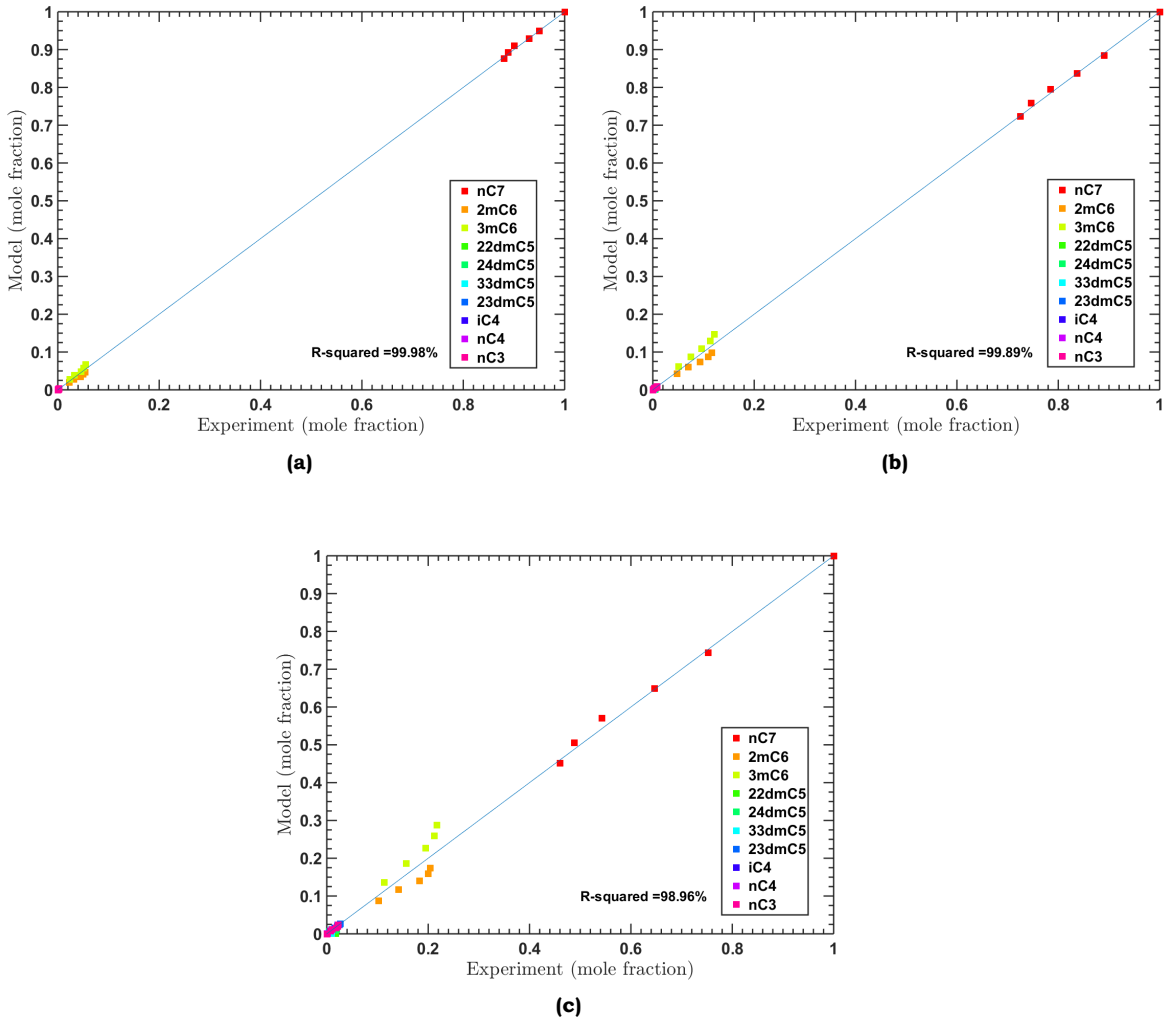

Figure 4.1: Parity plot of experimental observations vs. model computation of mole fractions at temperatures in the range 519K to 544K (a: 519K, b:531K, c:544K).

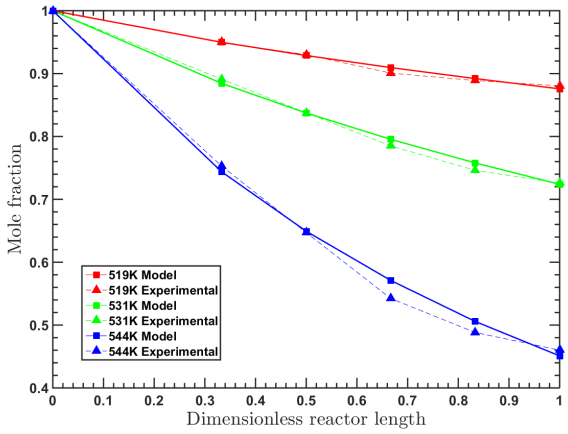

Figure 4.2: Concentration profile of n-Heptane obtained from model computation compared with experimental observations in the temperature range of 519K to 544K

Monobranched isomers of n-Heptane

2-Methylhexane (2mC6) and 3-Methylhexane (3mC6) are the two monobranched species involved in hydroisomerization and hydrocracking of n-Heptane. A distribution of these species is presented in Figures 4.3a and 4.3b. It is observed that out of all the species formed from converted n-Heptane, the monobranched isomers are highest in concentration, both experimentally as well by model. Experimental observations suggest almost equal concentration of 2-Methylhexane and 3-Methylhexane at all temperatures. At low reaction temperature of 531K, both 2-Methylhexane and 3-Methylhexane increase steadily. Both of the monobranched isomers undergo type C cracking reactions. In type C cracking reaction, neither a tertiary carbenium ion nor a branched alkene is formed. Hence the reaction rates for these reactions is very low. This is also a reason for high concentration of monobranched isomers of n-Heptane. Another reason for high concentration of these species is that these are the first isomerized products from n-Heptane as it enters the reactor. If given sufficient residence time or at higher reaction temperatures, these species will steadily decrease across the length of reactor as they will undergo branching and isomerization.

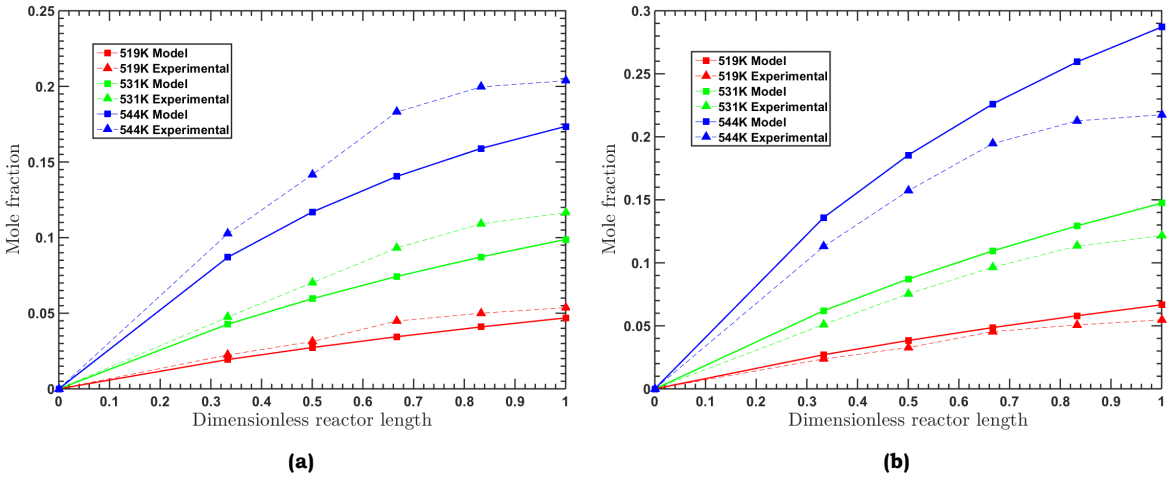

Figure 4.3: Distribution of monobranched isomers of heptane obtained from the model compared with experimental observations in the temperature range of 519K to 544K (a:2-Methylhexane, b:3-Methylhexane).

Dibranched isomers of n-Heptane

2,2-Dimethylpentane, 2,4-Dimethylpentane, 3,3-Dimethylpentane and 2,3-Dimethylpentane are the dibranched isomers observed in the reaction network. It is observed in Figures 4.4a, 4.4b, 4.4c and 4.4d, there is a very good agreement between experimental observations and model values for 2,3-Dimethylpentane and a considerable fitting for 2,4-Dimethylpentane. The order of concentration of dibranched isomers observed according to experiments is: 2,3-Dimethylpentane > 2,4-Dimethylpentane > 2,2-Dimethylpentane > 3,3-Dimethylpentane. However according to model, concentration of 2,2-Dimethylpentane and 2,4-Dimethylpentane is almost negligible in the system. One of the reasons for this might be the less contribution of these species to the object function due to very low concentrations and hence poor fitting with respect to these species. A solution to this problem could be increasing the scaling factor for these species. However, the scaling factor cannot be increased beyond a point as the solver will give arbitrary results in order to minimize the large object function. A better way to optimize for 2,2-Dimethylpentane and 3,3-Dimethylpentane is to analyze at higher reaction temperatures where the concentration of these species will be significant.

Among the dibranched isomers of heptane, 2,3-Dimethylpentane and 2,4-Dimethylpentane have the most stable carbenium ions as they are adequately stabilized by tertiary carbon atoms from all sides. At low reaction temperatures, concentrations of dibranched isomers increases steadily across the length of reactor. 2,3-Dimethylpentane undergoes type C cracking and 2,4-Dimethylpentane undergoes type B cracking. Hence among these two dibranched

isomers, 2,3-Dimethylpentane is observed in slightly higher quantities as compared to 2,4-Dimethylpentane. On the other hand, apart from being less stabilized, both 2,2-Dimethylpentane and 3,3-Dimethylpentane undergo type B cracking. This makes these two species the lowest formed products other than n-Butane.

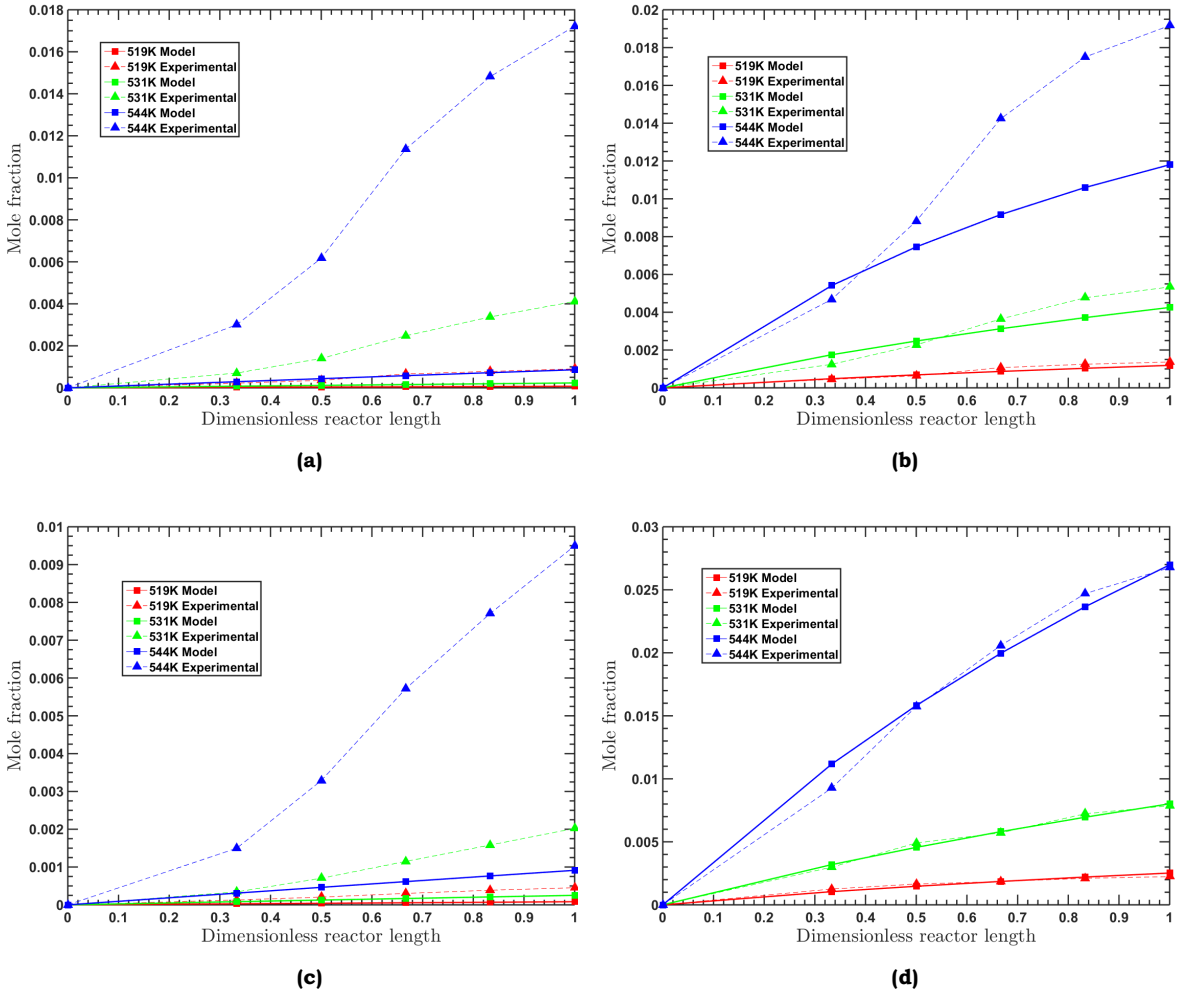

Figure 4.4: Distribution of dibranched isomers of heptane obtained from model computation compared with experimental observations in the temperature range of 519K to 544K (a:2,2-Dimethylpentane; b:2,4-Dimethylpentane; c:3,3-Dimethylpentane; d:2,3-Dimethylpentane). 2,4-Dimethylpentane and 2,3-Dimethylpentane fit well with the experimental results. The observed order of concentrations of dibranched isomers is 2,3-Dimethylpentane > 2,4-Dimethylpentane » 2,2-Dimethylpentane ≈ 3,3-Dimethylpentane.

Cracked products

The cracked products formed as a result of hydrocracking of heptanes are isobutane (iC4), n-butane (nC4) and propane (C3). Like in case of 2,4-Dimethylpentane and 2,3-Dimethylpentane, the model values of isobutane and propane are also in good agreement with experimental results. Among the cracked products, propane is present in highest proportions as it is formed in every cracking reaction either as an alkene or carbenium ion. Among butanes, n-Butane is formed almost negligibly as it is formed as a result of C-type beta scission reactions of 3-Methylhexane, 2-Methylhexane and 2,3-Dimethylhexane. As only secondary carbenium ions are formed in C-type cracking reactions, the rate of these reactions is significantly lower than B-type reactions [34]. Due to negligible presence of n-Butane, isobutane and propane are almost same in concentration. Similar to 2,2-Dimethylpentane and 3,3-Dimethylpentane, a poor fitting is also observed for propane due to its very low concentration in the system.

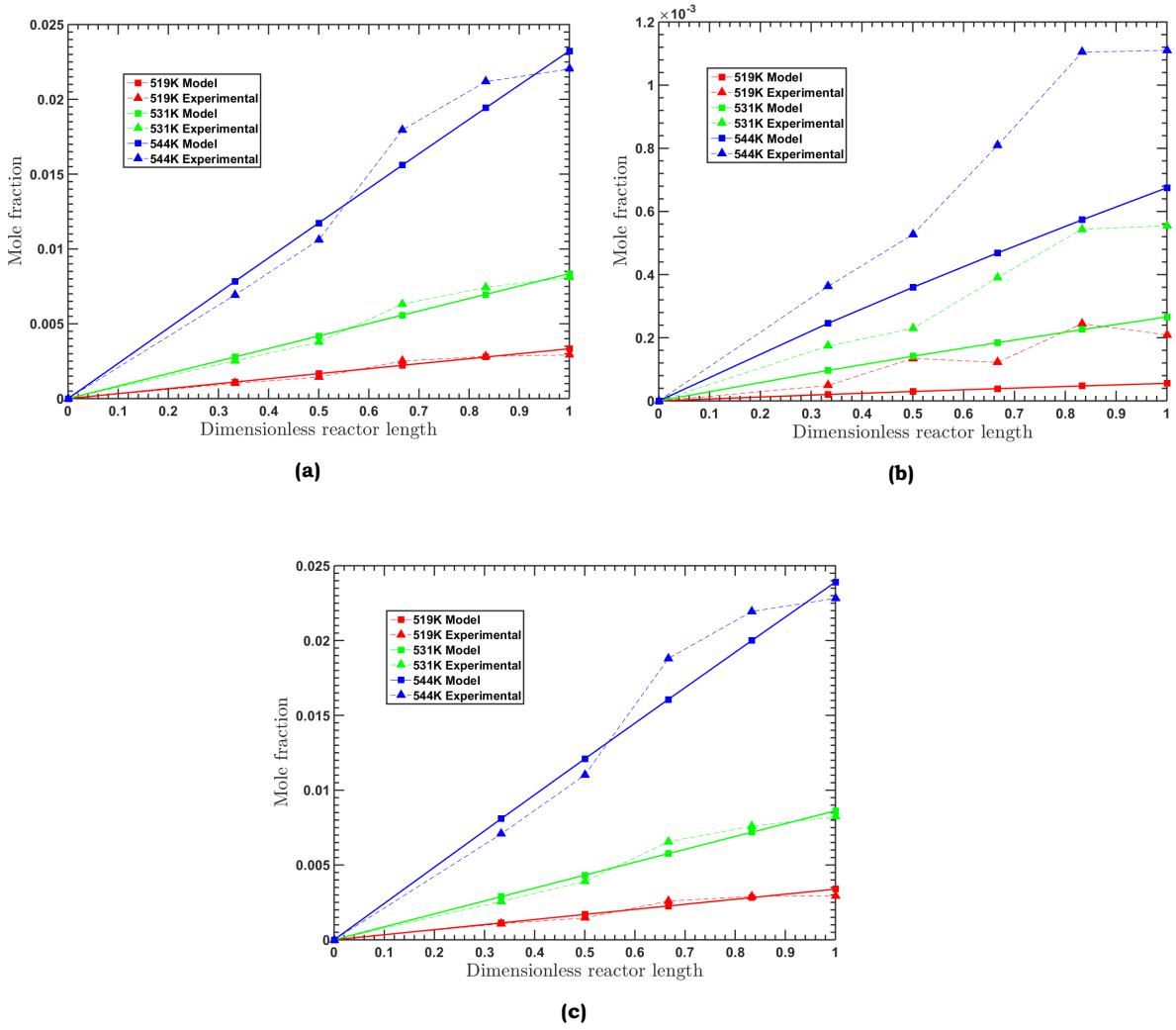

Figure 4.5: Distribution of cracked products as a result of cracking of heptane obtained from model computation compared with experimental observations in the temperature range of 519K to 544K (a:isobutane, b:n-Butane, c:propane). n-Butane is almost negligible in the system. Hence the concentration of isobutane and propane is almost same.

4.2. Parameter Estimations

Estimated values of single event rate coefficients as a result of fitting of model to experimental observations at different temperatures is presented in Table 4.1. In this table, it is observed that, the rates of reaction in general follow the trend $k_{hs} > k_{pr} \approx k_{de} > k_{ms} > k_{pcp} \approx k_{cr}$ (B type) $> k_{cr}$ (C type). This trend is consistent with the ones observed in literature [34, 34].

The rates of protonation, deprotonation and hydride shifts are almost always higher than isomerization and cracking reactions. The rate coefficients of protonation and deprotonation are in the same orders of magnitude except for $k_{de}(t,O_{ref7})$ and $k_{de}(s,O_{ref4})$. This is probably due to the additional stability of tertiary carbenium ions of heptanes. The deprotonation rate for tertiary carbenium ion of butane is directly proportional to $k_{de}(s,O_{ref4})$ as given in Equation 2.13. Due to the stability of tertiary carbenium ions of butane, the value of kinetic coefficient $k_{de}(s,O_{ref4})$ is also low.

For the isomerization rate coefficients, the rate of methyl shift is almost always higher than PCP decomposition which is consistent with literature trend. For the cracking reactions, reaction rates for type B reactions are always higher than type C reactions as there is conversion of secondary ions to tertiary ions in type B reactions [34]. This trend is also observed in the kinetic rate coefficients for cracking in Table 4.1.

Table 4.1: Estimated values of kinetic rate coefficients of elementary steps (in $\frac{kg_{cat}}{kmol.s}$) for protonation; in s^{-1} for other reactions). Overall, the values increase with temperature. The rates of reaction in general follow the trend $k_{hs} > k_{pr} \approx k_{de} > k_{ms} > k_{pcp} \approx k_{cr}$ (B type) > k_{cr} (C type)

Reaction type	Parameter type	Temperature		
		519K	**531K**	**544K**
Protonation	k_{pr}(s)	7.5E+08	1.8E+09	1.1E+10
	k_{pr}(t)	4.5E+08	2.3E+08	2.5E+06
Hydride shift	k_{hs}(s,s)	2.6E+11	6.7E+12	3.6E+14
	k_{hs}(s,t)	2.0E+14	7.6E+16	2.6E+16
	k_{hs}(t,t)	9.9E+15	5.6E+16	2.9E+17
Methyl shift	k_{ms}(s,s)	8.1E+06	1.1E+08	5.6E+07
	k_{ms}(s,t)	9.7E+09	5.0E+11	1.1E+13
PCP decomposition	k_{pcp}(s,s)	1.7E+06	7.4E+07	1.7E+09
	k_{pcp}(s,t)	1.0E+04	2.2E+06	2.4E+07
	k_{pcp}(t,t)	5.6E+02	3.7E+03	1.8E+05
Deprotonation	k_{de}s,O_{ref7}	4.1E+07	1.2E+09	1.3E+10
	k_{de}t,O_{ref7}	1.5E+02	3.5E+02	4.2E+04
	k_{de}s,O_{ref4}	2.0E+01	6.2E+02	1.6E+02
	k_{de}s,O_{ref3}	1.1E+04	2.1E+05	2.6E+05
Cracking	k_{cr}(B2)	3.7E+06	2.6E+07	1.7E+08
	k_{cr}(C)	3.7E-01	1.6E+02	1.2E+03
	k_{cr}(C)	3.0E+02	2.8E+04	1.2E+05
	k_{cr}(B1)	2.4E+08	6.5E+09	6.2E+10
	k_{cr}(C)	1.2E+05	7.0E+06	9.1E+07
	k_{cr}(B1)	1.5E+06	1.1E+08	1.2E+08

Average values of kinetic coefficients at 519K is presented and compared with each other in Figure 4.6 for visualization of trends. For better visualization, log of kinetic coefficients is presented on the y-axis. The values in this figure are average of values for (s,s), (s,t) and (t,t) reactions. However these average values cannot be indicative of exact trends as there is significant variation in values of each of these. For example the rate of methyl shift for (s,t) transition is higher than (s,s), as a transition from secondary ion to tertiary ion is thermodynamically favoured. The trend in Figure 4.6 can used to visualize that overall the rates of hydride shifts and methyl shifts are much higher than PCP decomposition and cracking reactions. In cracking, the rate of type B reactions is higher than type C reactions.

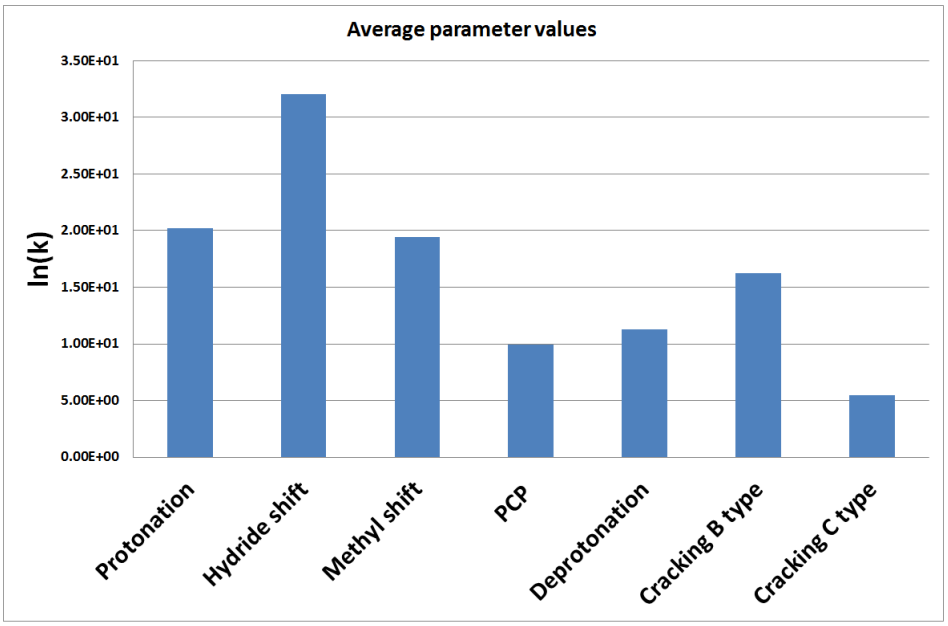

Figure 4.6: Average trend of kinetic rate constants. Overall, hydride shifts and methyl shifts are much faster than PCP decomposition and cracking reactions. In cracking, type B reactions are faster than type C reactions.

5

Conclusion

In this work, a model based on Single Event Microkinetics (SEMK) approach was developed for hydrocracking and hydroisomerization of n-Heptane in bifunctional catalyst. The SEMK approach takes into account contribution of every elementary step taking place in the vast web of reactions undergone by n-Heptane. It encompasses elementary step in the form of single reaction undergone by carbenium ion. In the model developed in this work, each hydrocarbon species is represented in the form of Binary Matrix (BM). The reaction network was developed by performing matrix operations on each of these BM's and storage of all reactions in an appropriate form. Thermodynamic constraints were used to reduce the number of independent rate constants to minimum possible number. Thus together with the data obtained from reaction network and independent rate constants, expressions were dervied for converison of n-Heptane and net rate of formation of all paraffin species. Expressions for model values for overall profile of partial pressures and concentrations were derived across the length of reactor. This model was fitted with experimental data to obtain values of rate constants for elementary reactions. After analyzing the results obtained from above described study, following conclusions can be drawn:

- Defining a hydrocarbon molecule in the form of Binary Matrix (BM) is an efficient way for carrying out elementary reactions in the form of matrix operations. However storage of these BM's and conversion into standardized form requires a lot of storage space and computational time.
- Genetic algorithm is an efficient algorithm for highly nonlinear optimization problems. However in this particular case, it suffers from the problem of reaching a local minima instead of global one and frequently getting stuck in local valleys in case small population sizes are provided. In order to reach a global minima, the population size can be increased, however for estimation of 20 parameters, the population size cannot be provided more than 10^4 as then excessively large random numbers are generated.
- The SEMK model predicts well for lower range reaction temperatures (till 544K in this work) and the estimated rate parameters follow the literature trend. However for higher temperatures, parameters other than rate coefficients of elementary reactions need to be taken into account to fully encompass the complexity of reactions.
- In the product distribution obtained as a result of hydroisomerization and hydrocracking of n-Heptane, the monobranched isomers are formed in highest proportion and 2-Methylhexane and 3-Methylhexane are almost same in proportion. In dibranched isomers, 2,3-Dimethylhexane and 2,4-Dimethylhexane are formed in large quantities as compared to 2,2-Dimethylhexane and 3,3-Dimethylhexane. The extent of cracking in the system increases as reaction temperature rises. n-Butane is formed in negligible amounts as a result of cracking. Isobutane and propane form the majority of the products and are almost equal amounts.

- Hydride shifts are the fastest reactions in carbenium ion chemistry for hydroisomerization and hydrocracking of straight chain alkanes. Methyl shifts are faster than PCP decomposition. B type cracking reactions are almost as fast as PCP decomposition reactions and C type cracking reactions are the slowest.

6

Recommendations

In this work, a model is created as a starting point for understanding reaction mechanism and product profile distribution for hydroisomerization and hydrocracking of n-Heptane in bifunctional catalysts via the SEMK approach. This model should serve as a base case and further modifications should be made to it to carry out advanced study. This advanced study can be understanding molecular shape selectivity or diffusion effects in bifunctional catalysts. Studies of this type have also been previously carried out [16, 44–46], but very few have been carried out using SEMK approach. The SEMK approach can be useful in understanding shape selectivity and diffusivity as it is fundamental in nature and encompasses every reaction taking place in the catalyst pores. Before carrying out these studies, recommendations to be considered are as follows:

- The reaction network should be generated with the help of standardized vectors for hydroisomerization and hydrocracking of n-Alkanes of higher order than 7. Using boolean matrices for the same is not convenient as it requires large storage space and computational time for the operations.
- The number and type of independent parameters should be chosen with care in order to preserve the dynamicity of the model. This majorly depends on the thermodynamic assumptions and constraints taken into account.
- The assumption that the concentration of components at successive nodes depend on the net rate of formation at previous node may prove inaccurate at high rates of formation at high temperatures. Hence, discretized scheme for partial pressure expressions at successive nodes should be implicit or higher order for computations at high reaction temperature. Althought this will affect the computational complexity and time required for calculations, in order to arrive at accurate results at high reaction temperatures, it is essential to derive a better discretized scheme.
- In the present work, there is no measure of credibility of values obtained by experimental results. In order to get accurate results, it is essential to know the confidence interval of experimental results. Hence it is strongly recommended to consider experimental results of multiple runs of the same experiment.
- The Genetic Algorithm (GA) used for optimization loses its ability to give a unique solution set for large set of unknown parameters (typically more than 15) and can get stuck in local minima for small population sizes. Hence multiple simulation runs are required to arrive at the unique solution set. Although the GA is a preferred choice for highly non-linear problems like in this work, other optimization algorithms like sequential quadratic programming can be considered which also take into account the gradience of the function for an unique solution set [47]. Another optimization algorithm which has proven to be better than GA for reaching a global optimum is stem cells algorithm based on evolutionary algorithms.

- Other recommendations to improve fitting of model are:
  - Reduce the number of parameters to be estimated by considering protonation and deprotonation reactions to be in equilibrium. By this approach, the values of these parameters can be readily computed by use of thermodynamic state functions.
  - Take into account more experimental observations in order to achieve better fitted values for large number of unknown parameters.

A

Model

A.1. Final indendent rate parameters

Table A.1 contain identities of species referred to in Table 2.6 for final independent unknown parameters.

Table A.1: Identities of species in Table 2.6

Symbol	Species
O_{ref7}	3-Methylhex-2-ene
O_{ref4}	But-2-ene
O_{ref3}	Propene
O_{cr1}	2-Methylprop-1-ene
O_{cr2}	But-2-ene
O_{cr3}	But-1-ene
O_{cr4}	Propene
O_{cr5}	Propene
R_1	2-Methylhexane-4+
R_2	2,2-Dimethylpentane-4+
R_3	3-Methylhexane-5+
R_4	2,3-Dimethylpentane-4+
R_5	2,4-Dimethylpentane-2+
R_{cr1}	Propane-2+
R_{cr2}	Propane-2+
R_{cr3}	Propane-2+
R_{cr4}	Butane-2+
R_{cr5}	2-Methylpropane-2+

B

Results and Discussions

B.1. Parameter estimations

The Arhenius plot is created by plotting $\frac{1}{T}$ vs. $\ln(k)$. A linear trendline fitted into this plot will have slope of $\frac{-E_a}{R}$ and intercept of $\ln(A)$ [48].

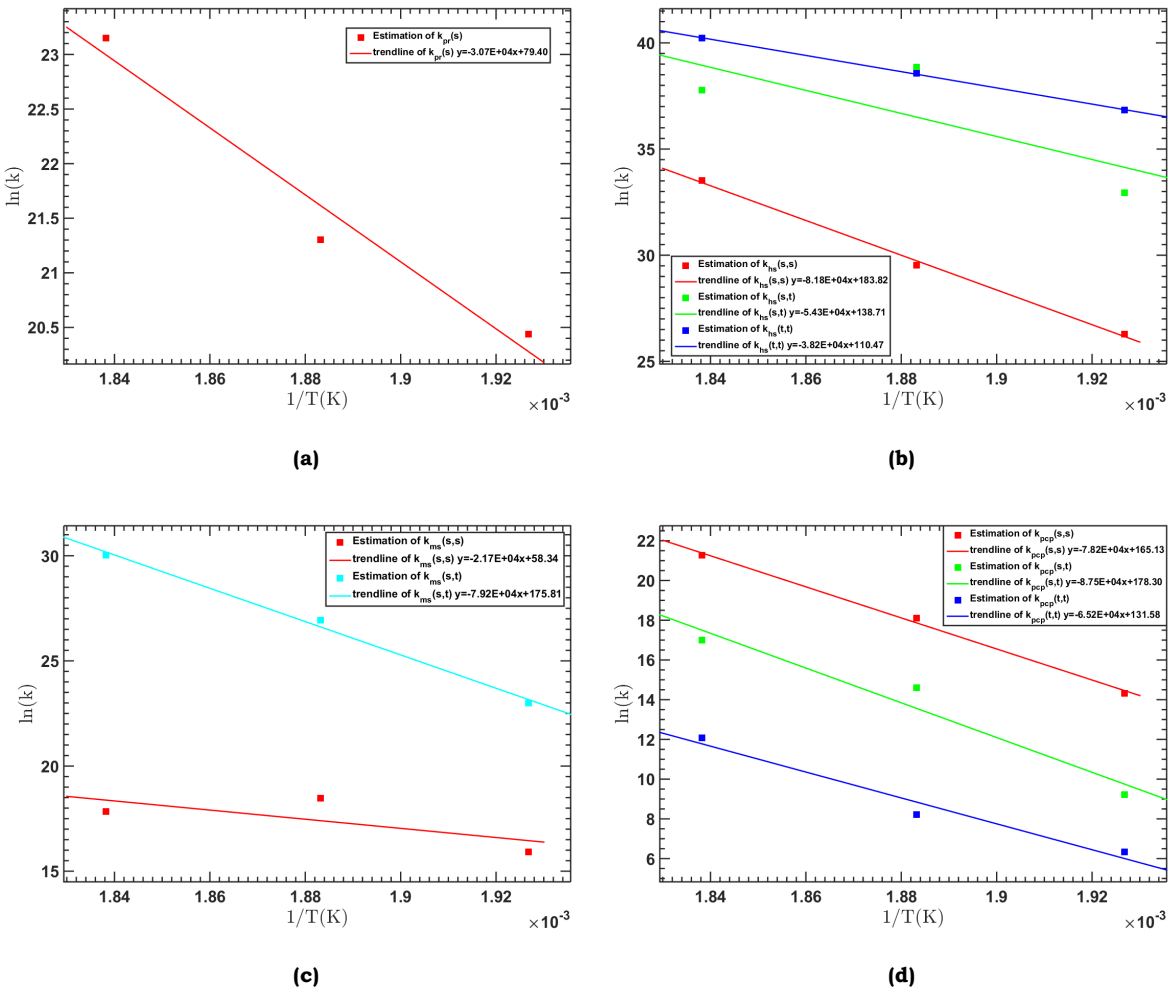

Figure B.1: Arhenius plots of selected rate parameters. The plots follow an almost linear trend and the slope of the graph is equal to $\frac{-E_{\text{activation}}}{R}$.

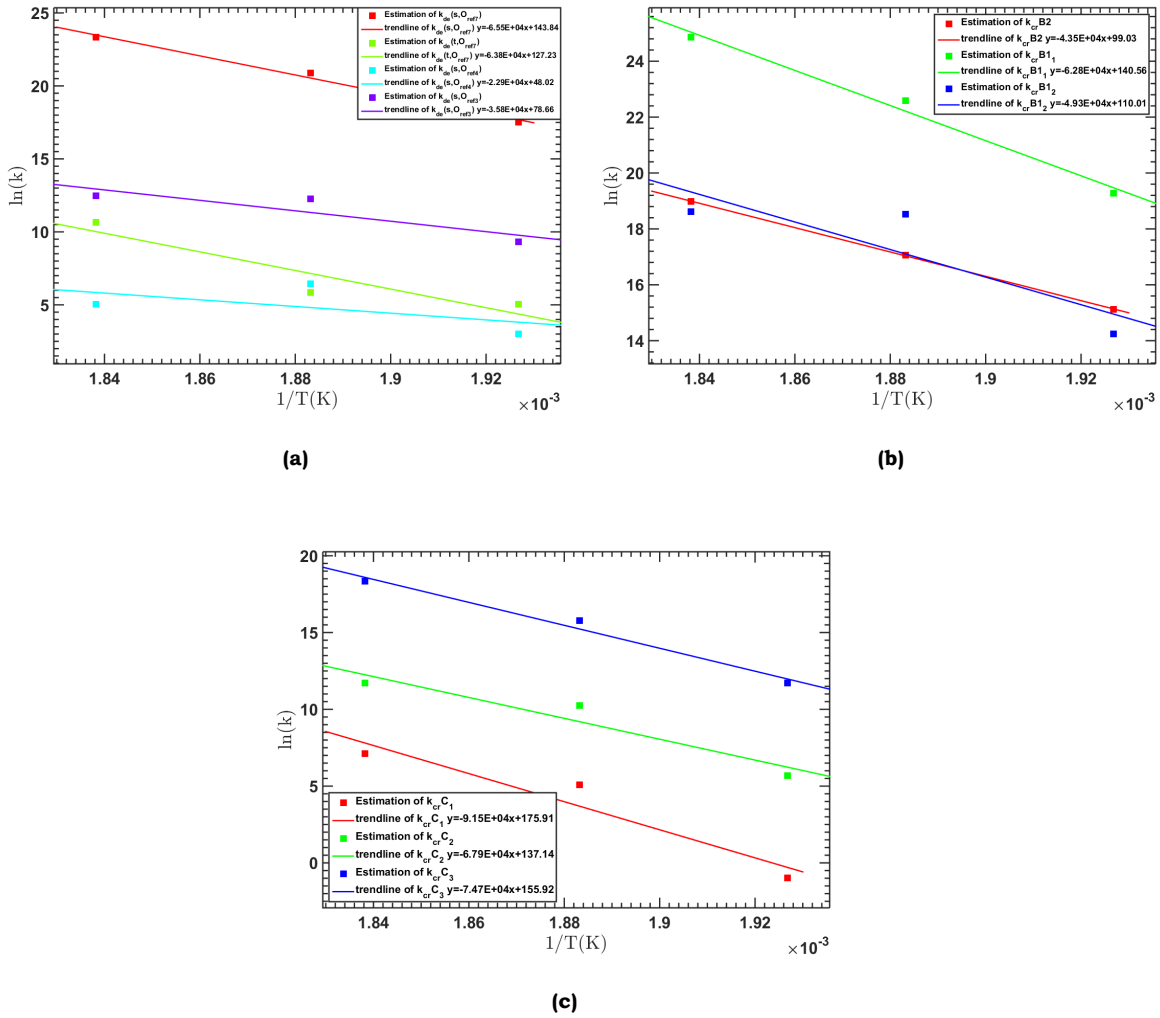

Figure B.2: Arhenius plots of selected rate parameters. The plots follow an almost linear trend and the slope of the graph is equal to $\frac{-E_{\text{activation}}}{R}$.

Bibliography

[1] C. Bouchy, G. Hastoy, E. Guillon, and J. Martens, *Fischer-tropsch waxes upgrading via hydrocracking and selective hydroisomerization,* Oil & Gas Science and Technology-Revue de l'IFP **64**, 91 (2009).

[2] J. Martens, R. Parton, L. Uytterhoeven, P. Jacobs, and G. Froment, *Selective conversion of decane into branched isomers: A comparison of platinum/zsm-22, platinum/zsm-5 and platinum/usy zeolite catalysts,* Applied catalysis **76**, 95 (1991).

[3] A. Corma, *Transformation of hydrocarbons on zeolite catalysts,* Catalysis letters **22**, 33 (1993).

[4] J. W. Ward, *Hydrocracking processes and catalysts,* Fuel Processing Technology **35**, 55 (1993).

[5] K.-C. Park and S.-K. Ihm, *Comparison of pt/zeolite catalysts for n-hexadecane hydroisomerization,* Applied Catalysis A: General **203**, 201 (2000).

[6] E. Vynckier and G. Froment, *Modeling of the kinetics of complex processes based upon elementary steps,* Kinetic and thermodynamic lumping of multicomponent mixtures **10**, 131 (1991).

[7] M. Guisnet, F. Alvarez, G. Giannetto, and G. Perot, *Hydroisomerization and hydrocracking of n-heptane on pth zeolites. effect of the porosity and of the distribution of metallic and acid sites.* Catalysis Today **1**, 415 (1987).

[8] J. F. Denayer, G. V. Baron, W. Souverijns, J. A. Martens, and P. A. Jacobs, *Hydrocracking of n-alkane mixtures on pt/h- y zeolite: Chain length dependence of the adsorption and the kinetic constants,* Industrial & engineering chemistry research **36**, 3242 (1997).

[9] M. Tromp, J. Van Bokhoven, M. G. Oostenbrink, J. Bitter, K. De Jong, and D. Koningsberger, *Influence of the generation of mesopores on the hydroisomerization activity and selectivity of n-hexane over pt/mordenite,* Journal of catalysis **190**, 209 (2000).

[10] F. De Gauw, J. Van Grondelle, and R. Van Santen, *Effects of single-file diffusion on the kinetics of hydroisomerization catalyzed by pt/h–mordenite,* Journal of Catalysis **204**, 53 (2001).

[11] H. Kumar, *Mechanistic kinetic modeling of the hydrocracking of complex feedstocks*, Ph.D. thesis, Texas A&M University (2006).

[12] J. F. Denayer, J. A. Martens, P. A. Jacobs, J. W. Thybaut, G. B. Marin, and G. Baron, *Influence of the zeolite composition on the hydro-isomerisation and hydrocracking of alkanes on pt/usy zeolites: modelling of the reaction kinetics using an adsorption–reaction approach,* Applied Catalysis A: General **246**, 17 (2003).

[13] G. Froment, *Kinetics of the hydroisomerization and hydrocracking of paraffins on a platinum containing bifunctional y-zeolite,* Catalysis Today **1**, 455 (1987).

[14] J. Martens, P. Jacobs, and J. Weitkamp, *Attempts to rationalize the distribution of hydrocracked products. i qualitative description of the primary hydrocracking modes of long chain paraffins in open zeolites,* Applied Catalysis **20**, 239 (1986).

[15] G. Martens, G. Marin, J. Martens, P. Jacobs, and G. Baron, *A fundamental kinetic model for hydrocracking of c 8 to c 12 alkanes on pt/us–y zeolites,* Journal of catalysis **195**, 253 (2000).

[16] A. Soualah, J.-L. Lemberton, L. Pinard, M. Chater, P. Magnoux, and K. Moljord, *Hydroisomerization of long-chain n-alkanes on bifunctional pt/zeolite catalysts: Effect of the zeolite structure on the product selectivity and on the reaction mechanism,* Applied Catalysis A: General **336**, 23 (2008).

[17] S. M. Jacob, B. Gross, S. E. Voltz, and V. W. Weekman, *A lumping and reaction scheme for catalytic cracking,* AIChE Journal **22**, 701 (1976).

[18] C. Laxminarasimhan, R. Verma, and P. Ramachandran, *Continuous lumping model for simulation of hydrocracking,* AIChE Journal **42**, 2645 (1996).

[19] D. Orochko, I. Y. Perezhigina, S. Rogov, M. Rysakov, and G. Chernakova, *Applied overall kinetics of hydrocracking of heavy petroleum distillates,* Chemistry and Technology of Fuels and Oils **6**, 561 (1970).

[20] S. Quader, S. Singh, W. Wiser, and G. Hill, *Hydrocracking of petroleum oil,* J. Inst. Petrol **56**, 187 (1970).

[21] Y. M. Zhorov, P. GM, T. GM, S. Kuzmin, and Z. SM, *Chemical scheme and structure of mathematical description of hydrocracking,* INTERNATIONAL CHEMICAL ENGINEERING **11**, 256 (1971).

[22] M. Steijns and G. F. Froment, *Hydroisomerization and hydrocracking. 3. kinetic analysis of rate data for n-decane and n-dodecane,* Industrial & Engineering Chemistry Product Research and Development **20**, 660 (1981).

[23] V. W. Weekman and D. M. Nace, *Kinetics of catalytic cracking selectivity in fixed, moving, and fluid bed reactors,* AIChE Journal **16**, 397 (1970).

[24] B. E. Stangeland, *A kinetic model for the prediction of hydrocracker yields,* Industrial & Engineering Chemistry Process Design and Development **13**, 71 (1974).

[25] D. K. Liguras and D. T. Allen, *Structural models for catalytic cracking; model compound reactions,* Industrial and Engineering Chemistry Research;(USA) **28** (1989).

[26] R. J. Quann and S. B. Jaffe, *Structure-oriented lumping: describing the chemistry of complex hydrocarbon mixtures,* Industrial & engineering chemistry research **31**, 2483 (1992).

[27] M. A. Baltanas, K. K. Van Raemdonck, G. F. Froment, and S. R. Mohedas, *Fundamental kinetic modeling of hydroisomerization and hydrocracking on noble-metal-loaded faujasites. i: Rate parameters for hydroisomerization,* Industrial & Engineering Chemistry Research **28**, 899 (1989).

[28] P. Clymans and G. Froment, *Computer-generation of reaction paths and rate equations in the thermal cracking of normal and branched paraffins,* Computers & chemical engineering **8**, 137 (1984).

[29] L. Hillewaert, J. Dierickx, and G. Froment, *Computer generation of reaction schemes and rate equations for thermal cracking,* AIChE Journal **34**, 17 (1988).

[30] M. A. Baltanas and G. F. Froment, *Computer generation of reaction networks and calculation of product distributions in the hydroisomerization and hydrocracking of paraffins on pt-containing bifunctional catalysts,* Computers & chemical engineering **9**, 71 (1985).

[31] G. D. Svoboda, E. Vynckier, B. Debrabandere, and G. F. Froment, *Single-event rate parameters for paraffin hydrocracking on a pt/us-y zeolite,* Industrial and Engineering Chemistry Research **34** (1995).

[32] T.-Y. Park and G. F. Froment, *Kinetic modeling of the methanol to olefins process. 1. model formulation,* Industrial & Engineering Chemistry Research **40**, 4172 (2001).

[33] J. M. Martinis and G. F. Froment, *Alkylation on solid acids. part 2. single-event kinetic modeling,* Industrial & engineering chemistry research **45**, 954 (2006).

[34] E. Blomsma, J. Martens, and P. Jacobs, *Mechanisms of heptane isomerization on bifunctional pd/h-beta zeolites,* Journal of catalysis **159**, 323 (1996).

[35] H. Eyring, *The activated complex and the absolute rate of chemical reactions.* Chemical Reviews **17**, 65 (1935).

[36] E. S. Domalski and E. D. Hearing, *Estimation of the thermodynamic properties of hydrocarbons at 298.15 k,* Journal of physical and chemical reference data **17**, 1637 (1988).

[37] D. Bishop and K. Laidler, *Statistical factors for chemical reactions,* Transactions of the Faraday Society **66**, 1685 (1970).

[38] R. A. Alberty and C. A. Gehrig, *Standard chemical thermodynamic properties of alkene isomer groups,* Journal of physical and chemical reference data **14**, 803 (1985).

[39] G. Mills, H. Heinemann, T. Milliken, and A. Oblad, *(houdriforming reactions) catalytic mechanism,* Industrial & Engineering Chemistry **45**, 134 (1953).

[40] *Online zeolites database,* http://www.iza-structure.org/databases/, accessed: 2017-04-25.

[41] *Genetic Algorithm description,* https://en.wikipedia.org/wiki/Genetic_algorithm, accessed: 2017-04-20.

[42] *Genetic Algorithm MATLAB,* https://nl.mathworks.com/discovery/genetic-algorithm.html, accessed: 2017-04-20.

[43] *R-squared description,* https://en.wikipedia.org/wiki/Coefficient_of_determination, accessed: 2017-04-25.

[44] M. C. Claude, G. Vanbutsele, and J. A. Martens, *Dimethyl branching of long n-alkanes in the range from decane to tetracosane on pt/h–zsm-22 bifunctional catalyst,* Journal of catalysis **203**, 213 (2001).

[45] M. C. Claude and J. A. Martens, *Monomethyl-branching of long n-alkanes in the range from decane to tetracosane on pt/h-zsm-22 bifunctional catalyst,* Journal of Catalysis **190**, 39 (2000).

[46] B. Smit and T. L. Maesen, *Towards a molecular understanding of shape selectivity,* Nature **451**, 671 (2008).

[47] *Sequential Quadratic Programming description,* https://en.wikipedia.org/wiki/Sequential_quadratic_programming, accessed: 2017-04-25.

[48] *Arhenius plots wikipedia description,* https://en.wikipedia.org/wiki/Arrhenius_plot, accessed: 2017-04-25.